Advances in Biological Regulation 80 (2021) 100808

Contents lists available at ScienceDirect

Advances in Biological Regulation

journal homepage: www.elsevier.com/locate/jbior

Characterization of pepcan-23 as pro-peptide of RVD-hemopressin (pepcan-12) and stability of hemopressins in mice

Sandra Glasmacher [a,b], Jürg Gertsch [a,*]

[a] Institute of Biochemistry and Molecular Medicine, University of Bern, CH-3012, Bern, Switzerland
[b] Graduate School for Cellular and Biomedical Sciences (GCB), University of Bern, Switzerland

ARTICLE INFO

Keywords:
Peptides
Hemopressin
Cannabinoid receptors
Pepcans
Metal binding

ABSTRACT

Hemopressins ((x)-PVNFKLLSH) or peptide endocannabinoids (pepcans) can bind to cannabinoid receptors. RVD-hemopressin (pepcan-12) was shown to act as endogenous allosteric modulator of cannabinoid receptors, with opposite effects on CB1 and CB2, respectively. Moreover, the N-terminally elongated pepcan-23 was detected in different tissues and was postulated to be the pro-peptide of RVD-hemopressin. Currently, data about the pharmacokinetics, tissue distribution and stability of hemopressin-type peptides are lacking. Here we investigated the secondary structure and physiological role of pepcan-23 as precursor of RVD-hemopressin. We assessed the metabolic stability of these peptides, including hemopressin. Using LC-ESI-MS/MS, pepcan-23 was measured in mouse tissues and human whole blood (~50 pmol/mL) and in plasma was the most stable endogenous peptide containing the hemopressin sequence. Using peptide spiked human whole blood, mouse adrenal gland and liver homogenates demonstrate that pepcan-23 acts as endogenous pro-peptide of RVD-hemopressin. Furthermore, administered pepcan-23 converted to RVD-hemopressin in mice. In circular dichroism spectroscopy, pepcan-23 showed a helix-unordered-helix structure and efficiently formed complexes with divalent metal ions, in particular Cu(II) and Ni(II). Hemopressin and RVD-hemopressin were not bioavailable to the brain and showed poor stability in plasma, in agreement with their overall poor biodistribution. Acute hemopressin administration (100 mg/kg) did not modulate endogenous RVD-hemopressin/pepcan-23 levels or influence the endocannabinoid lipidome but increased 1-stearoyl-2-arachidonoyl-sn-glycerol. Overall, we show that pepcan-23 is a biological pro-peptide of RVD-hemopressin and divalent metal ions may regulate this process. Given the lack of metabolic stability of hemopressins, administration of pepcan-23 as pro-peptide may be suitable in pharmacological experiments as it is converted to RVD-hemopressin *in vivo*.

1. Introduction

The endocannabinoid system (ECS) was discovered as a consequence of the elucidation of Δ^9-tetrahydrocannabinol (Δ^9-THC) as the major psychoactive natural product of *Cannabis sativa* L (Matsuda et al., 1990; Mechoulam and Gaoni, 1964; Mechoulam and Parker, 2013). The ECS is an essential lipid signaling network in mammals, comprising the arachidonate (AA)-derived endocannabinoids (eCBs) 2-arachidonoylglycerol (2-AG) and N-arachidonoylethanolamine (anandamide, AEA), the corresponding enzymes for

* Corresponding author. Institute of Biochemistry and Molecular Medicine, University of Bern, Bühlstrasse 28, CH-3012, Bern, Switzerland.
E-mail address: gertsch@ibmm.unibe.ch (J. Gertsch).

https://doi.org/10.1016/j.jbior.2021.100808
Received 1 February 2021; Received in revised form 2 March 2021; Accepted 18 March 2021
Available online 24 March 2021

their biosynthesis and degradation, as well as their G-protein coupled receptors (GPCRs) CB1 and CB2. The eCBs are connected to the arachidonate-prostaglandin axis and non-selectively and tissue-dependently activate CB1, CB2 or GPR55 receptors, but likewise, they modulate different ion channels and intracellular receptors (Lenman and Fowler, 2007; Morales et al., 2017; Ryberg et al., 2007; Sigel et al., 2011; Yévenes and Zeilhofer, 2011; Zygmunt et al., 1999). More recently, peptides derived from the hemopressin sequence PVNFKLLSH (present in the α-hemoglobin HBA1/2 and Hba-x gene loci) were reported to interact with cannabinoid (CB) receptors (Bauer et al., 2012; Emendato et al., 2018; Gelman and Fricker, 2010; Gomes et al., 2009; Petrucci et al., 2017; Rioli et al., 2003; Scrima et al., 2010; Straiker et al., 2015; Wei et al., 2020). Among these peptides, an endogenous peptide called RVD-hemopressin or pepcan-12 (nomenclature based on the N-terminal extension) was shown to act as potent (nanomolar) allosteric modulator of the CB receptors *in vitro*. At CB1 receptors this peptide behaved as negative allosteric modulator (NAM) whereas at CB2 receptors it showed effects of a positive allosteric modulator (PAM) (Bauer et al., 2012; Petrucci et al., 2017; Straiker et al., 2015). More recently, it was demonstrated that the endogenous peptides RVD-hemopressin and pepcan-23 are localized in noradrenergic neurons in the brain, as well as in the adrenal glands (Hofer et al., 2015; Petrucci et al., 2017). Because of the restricted localization and the relatively small amounts of these neuropeptides in blood and tissues, independent of the absolute amounts of hemoglobin, their generation seems to be independent of α-hemoglobin degradation. Pepcan-23 may be generated from cryptic localized expression of the HBA2 gene and post-translational processing (Hofer et al., 2015; Wei et al., 2020). Given the relative abundance of pepcan-23 and its lack of CB receptor binding (Bauer et al., 2012; Petrucci et al., 2017), it was previously postulated that this peptide could be the pro-peptide of RVD-hemopressin (pepcan-12). In agreement with this hypothesis, pepcan-23 tissue levels were increased simultaneously with RVD-hemopressin and eCBs during ischemia-reperfusion injury (IRI) and inflammation in mice (Petrucci et al., 2017). However, the role of pepcan-23 remains unclear. Despite the lack of knowledge about the biological stability of these peptides, hemopressin and RVD-hemopressin are increasingly used in pharmacological experiments (*vide infra*). The data obtained in these studies need to be discussed and re-evaluated based on the biological stability of hemopressins. Different studies with hemopressin and RVD-hemopressin have been conducted *in vitro* and *in vivo*, in various species and routes of administration, including oral (p.o.), intraperitoneal (i.p.), and intravenous (i.v.) (Aygun et al., 2020; Blais et al., 2005; Camargo et al., 2020; Dale et al., 2005; Dodd et al, 2010, 2013; El Swefy et al., 2016; Ferrante et al., 2017; Fogaça et al., 2015; Hama and Sagen, 2011a, 2011b; Heimann et al., 2007; Leone et al., 2017; Li et al., 2016; Lippton et al., 2006; Mahmoud et al., 2014; Pan et al., 2014; Petrovszki et al., 2012; Recinella et al., 2018; Rioli et al., 2003; Tanaka et al., 2014; Toniolo et al., 2014; Zhang et al., 2016; Zhou et al., 2012). To date, the structure and stability of pepcan-23 has not yet been investigated in pharmacological experiments. In the present study, we employed the power of liquid chromatography tandem mass spectrometry (LC-MS/MS) to quantify the stability and bioavailability of hemopressin, RVD-hemopressin and pepcan-23 in different biological tissues, both *in vivo* and *ex vivo*. We address the hypothesis that pepcan-23 is the physiological pro-peptide of RVD-hemopressin (pepcan-12) *in vivo*. Based on a previous report on hemopressin peptide metal-binding (Remelli et al., 2016), we further postulated that divalent metal cations may stabilize the secondary structure of pepcan-23 in physiological environment and influence its metabolic stability. Using circular dichroism (CD) spectroscopy and mass spectrometry (MS) we studied the interaction of the peptides with different divalent metal ions and investigated the metabolic stability of each hemopressin, RVD-hemopressin and pepcan-23 in serum, plasma and blood, as well as the potential effect of hemopressin on the ECS *in vivo*. Our data substantiate that pepcan-23 acts as pro-peptide of RVD-hemopressin and we show that this peptide has superior biological stability than the shorter hemopressins. Possible structural reasons for this finding are discussed. Overall, our study provides first important insights into the biological role of pepcan-23 in the biosynthetic regulation of RVD-hemopressin, but also red-flags shorter pepcans and hemopressin from being used as pharmacological agents in animal studies.

2. Materials and methods

2.1. Materials and reagents

Peptides (purity >95%) were obtained customized from GeneCust. The peptide internal standard was synthesized by SHBC. All general compounds, salts and buffer were purchased from Sigma-Aldrich and Fluka: Tris(hydroxymethyl)aminomethane hydrochloride (Tris-HCl), ethylene-diaminetetraacetic acid (EDTA), trifluoroethanol (TFE) and metal salts ($CuCl_2$, $NiCl_2$, $ZnCl_2$, $CaCl_2$, $MgCl_2$ and $MnCl_2$), phosphate buffer saline (PBS), sodium dihydrogenphosohate dihaydrate, sodium phosphate dibasic dihydrate. Phosphate buffer (PB buffer) was prepared in house using sodium dihydrogenphosohate dihaydrate and sodium phosphate dibasic dihydrate. Bicinchoninic acid (BCA) colorimetric assay was obtained from Pierce Biotechnology, ThermoScientific™. Solvents for MS experiments were purchased in HPLC and analytical grade from Sigma-Aldrich and VWR Scientific. MilliQ water (18.2 MΩ x cm) was obtained from an ELGA Purelab Ultra Genetic system. The protease inhibitor cocktail (PIC) (Complete Ultra Tablets Mini) from Roche was used. Solid-phase extraction (SPE) cartridges (Oasis® HLB, 1 cc, 30 mg) were purchased from Waters™. Plastic extraction tubes (2 mL) and chrome-steel beads (2.3 mm dia) were purchased from XXTuff Microvials, BioSpec.

2.2. ESI mass spectrometry

Electrospray ionization mass spectrometry (ESI-MS) flow injection analyses in presence or absence of metals were carried out on 4000 QTrap mass spectrometer equipped with ESI probe (AB Sciex Concord, Ontario, Canada). Data acquisition and analysis were performed using the Analyst software version 1.6 (AB Sciex Concord, Ontario, Canada). The turbo ion spray interface was operated in positive mode. The parameters of the ion source using nitrogen as curtain gas were as follows: Ion spray voltage 2000 V, temperature 650 °C, curtain gas 25 psi, GS1 50 psi and GS2 50 psi. The entrance potential and collision cell exit potential were set to 10 V. Spectra

were acquired in the 70-2800 m/z range using Q1 MS in positive mode. Peptides (0.6 mM) were incubated in milliQ water in the absence or presence of divalent metal salts (peptide/metal (Cu(II) or Ni(II)) ratio 1:1, 1:2, 1:10), diluted to 50% acetonitrile (ACN) and subjected to the LC-MS. Sample (50 μL) was injected into the LC-MS using a constant flow of 1:1 ACN/water containing 0.1% formic acid and a flow rate of 0.2 mL/min for 5 min. To identify the characteristic signals for relevant metal ion-peptide complexes, the solvent system and the peptide without metal were recorded as control spectra.

2.3. Peptide sample preparation and extraction

For peptide extraction from tissues, a gentle extraction method consisting of protein precipitation (PPT) and solid-phase extraction was used. Peptides were extracted from tissues as described previously with minor adaptations (Petrucci et al., 2017). In brief, frozen tissue was weighed, transferred into extraction tubes containing two steel beads. Depending on the tissue, two to four volumes ice-cold water containing PIC were added. Homogenization was carried out using a bead beater (Mini-BeadBeater-24, BioSpec, Oklahoma, USA). PPT of an aliquot of the sample homogenate was performed using acetonitrile (1:1, v/v), followed by the addition of the internal standard (1 μg/mL for 4000 QTrap, 0.1 μg/mL for 5500 QTrap). PPT was facilitated by keeping the samples on ice for 10 min, followed by vigorous vortexing and sonication for 10 min in an ice-cold ultrasound bath. Subsequently, samples were centrifuged at 16 000 *g* for 10 min at 4 °C and the supernatant was diluted to 10% ACN with milliQ water. Samples were then subjected to SPE. For whole blood, serum, and plasma samples, protein precipitation was performed using an equal part of ACN, vortexed and IS was added. The samples were then 5 min sonicated for homogenization prior to subsequent extraction steps, as mentioned above.

2.4. Solid-phase extraction (SPE)

Sample cleanup and concentration of peptides was performed with a SPE protocol using Oasis® HLB cartridges. The sorbent of the cartridge was activated and conditioned using 1 mL methanol, followed by equilibration with 10% ACN. Afterward, the sample was loaded on the cartridge and the sorbent was washed with 500 μL water. Analytes were eluted using 850 μL 70% ACN and the eluate was dried under vacuum in a SpeedVac. Prior LC-MS/MS measurements, samples were reconstituted in 10% ACN.

2.5. Acidic extraction of hemopressin and pepcan-23 from human whole blood

Peptides from human whole blood were extracted by adding one volume (v/v) of acid (100 mM acetic acid/0.1 M formic acid/10 mM hydrochloric acid (HCl)). For hot extraction, blood was incubated for 20 min at 100 °C. Extraction was performed as described in 2.3 and 2.4.

2.6. LC-ESI-MS/MS measurements

Analyses were conducted on a 4000 QTrap mass spectrometer equipped with ESI probe (AB Sciex Concord, Ontario, Canada) connected to a LC-20AD Shimadzu UFLC system (Shimadzu Corporation, Kyoto, Japan) as previously described (Petrucci et al., 2017). In brief, analytes were measured in multiple reaction-monitoring mode (MRM). The chromatographic separation of peptides (molecular weight ranges from 1054 to 2597 Da) was performed on a C8 column (3 μm, 50 × 2 mm, ReproSil-Pur Basic®, Dr. A. Maisch, High Performance LC-GMBH, Ammerbuch, Germany) maintained at 40 °C. LC was performed using water 0.1% formic acid and ACN 0.1% formic acid as mobile phase (schematic representation in Supplementary Fig. 1). Peptides were eluted using a linear gradient from 2% to 80% organic solvent over 19 min with a flow rate of 0.3 mL/min. The analytical range for RVD-hemopressin and pepcan-23 with this method was 56–2000 ng/mL. As previously reported, values obtained for R^2 were higher than 0.94 (Hofer et al., 2015; Petrucci et al., 2017).

Measurements and validation of the new peptide LC-MS/MS method were performed on a more sensitive 5500 QTrap mass spectrometer equipped with an ESI probe (AB Sciex Concord, Ontario, Canada) and connected to an ExionLC AC UHPLC system (AB Sciex Concord, Ontario, Canada). The instrument parameters were: IS +2500 V, source temperature 650 °C, curtain gas 40 psi, GS1 70 psi and GS2 60 psi, entrance potential and collision cell exit potential 10 V. Autosampler was maintained at 4 °C. The MRM transitions used for the quantification of hemopressin, RVD-hemopressin, pepcan-23, and the internal standard (IS) RVDPVNFKFL(5,5,5-D3)SH are shown in the Supplementary Table 1. The chromatographic separation of the peptides was performed as described previously (Petrucci et al., 2017).

2.7. Pepcan quantification and method validation

Because RVD-hemopressin, and pepcan-23 are endogenous compounds, diluted tissues were used as matrix for the calibration and the endogenous background concentration of each analytes in the matrix was subtracted from the concentrations of the spiked calibrants (Thakare et al., 2016). Peptides were quantified using Analyst 1.6 (AB Sciex) based on the calculated analyte ratio (peak area of each analyte/peak area of IS). The slope, intercept, and regression coefficient of the calibration were determined, and data were analyzed using linear regression. The calibrants were prepared by spiking diluted matrix with the freshly prepared stock of peptides due to the low freeze/thaw stability of the peptides in solution (Supplementary Table 2). R^2 ranged from 0.95 to 0.99. A representative validation of the most relevant parameters was performed using diluted blood as matrix. Validation samples were prepared at three quality control (QC) levels for all the peptides: low (LQC 6.9 ng/mL), middle (MQC 52 ng/mL), and high (HQC 395 ng/mL) spanning

the entire calibration range (Supplementary Tables 1–5).

2.8. Quantification of endocannabinoids by LC-MS/MS

Collected and snap-frozen tissues were weighed and extracted as previously reported (Chicca et al., 2017). In brief, if both peptides, eCBs, and lipids were quantified in the same sample, tissues were homogenized in water containing PIC instead of 0.1 M formic acid solution. 20-50 mg was transferred to glass extraction tubes containing ice cold 1.5 mL ethyl acetate/hexane (9:1) 0.1% formic acid solutions and the ISs. The ratio of the organic and aqueous phase was adjusted to 3:1 organic solvent and aqueous phase containing the homogenate. The extraction tubes were rigorously vortexed for 30 s, followed by 10 min a sonication step in a cold bath. Subsequently, samples were centrifuged 1600 *g* for 10 min at 4 °C and placed on dry ice to allow the aqueous layer to freeze. The upper organic phase was recovered in plastic tubes and was dried to completeness under vacuum. The samples were reconstituted in either 35 μL or 50 μL 80% ACN in water, submitted to the LC-MS, and 10 μL were injected for measurement. The LC-MS/MS parameters and conditions were as previously described (Chicca et al., 2017; Gachet et al., 2015; Schuele et al., 2020).

2.9. Blood collection, plasma and serum generation

For whole blood and plasma experiments, blood was collected in EDTA tubes (VACUETTE®) provided by the local blood bank (Blutspendezentrum Bern, Switzerland) and processed in the lab under the BAFU license No A141370. For serum, whole blood from healthy male and female donors was collected in serum tubes (without any anticoagulant) and allowed to clot overnight. Whole blood was centrifuged for 15 min at 1000 *g* in a cooled centrifuge to obtain plasma and serum in house. Acceleration and brake were set to zero to avoid the disruption of phase separation and breaking of cells. The supernatant (plasma or serum) was recovered without disturbing the cellular fraction and aliquoted into 2 mL tubes (Eppendorf). For pooling whole blood only compatible blood types were used.

2.10. Circular dichroism (CD) spectroscopy

CD spectra were recorded using Jasco J-715 spectrometer equipped with a PFD-350 S temperature controller and a PS-150 J power supply. All experiments were measured using a Hellma Suprasil R 100-QS 0.1 cm cuvette. Stock solutions of the peptides (2 mg/mL) were freshly prepared immediately before the experiment using degassed milliQ water and diluted to the final concentration using degassed phosphate buffer (PB) (10 mM PB buffer final concentration). For the TFE and pH studies, 200 μg/mL peptides were used. For the metal binding experiments, 1 mM peptide and 1.1 mM metal (Cu(II) or Ni(II)) were used. The pH of the PB buffer was adjusted by mixing Na_2HPO_4 buffer and NaH_2PO_4 buffer accordingly. The prepared buffers and solutions were degassed before use to reduce background noise in the measurement. For the solvent dependent studies (induction of secondary structure, pH studies) PB buffer at various pH (pH 4.5, pH 7.4, pH 9), containing different TFE (0–100%) solutions, or in the presence of Cu(II) or Ni(II) were used. The parameters of the instrument were as followed: temperature 20 °C, range of measurement 185-260 nm (pH and TFE studies) and 200-700 nm (metal binding studies), scan rate set to 10 nm/min, or 20 nm/min, pitch 0.5–1 nm, response 16 s, nitrogen flow was kept above 8 L/min and samples were subjected to at least two accumulations per measurement. The baseline of each used buffer or solvent was recorded under the same conditions and subtracted manually for data analysis. Between each measurement, the cuvettes were washed with milliQ water, 1 M HCl, milliQ water, then equilibrated with the buffer used for the next measurement. The obtained data was analyzed and processed by Dichroweb using CONTIN LL analysis program and reference set three (Lobley et al., 2002; Provencher and Glöckner, 1981; Van Stokkum, I. H., Spoelder, H. J., Bloemendal, M., Van Grondelle, R., & Groen, 1990; Whitmore and Wallace, 2008, 2004). Final data was plotted using GraphPad Prism 9.

2.11. Stability studies

Whole blood, plasma, and serum stability of hemopressin, RVD-hemopressin, and pepcan-23 was assessed in an *ex vivo* stability assay. Peptides (2 μM) were added separately to each matrix which was incubated at 37 °C, 300 rpm on the thermoshaker for up to 120 min. An aliquot was taken at the indicated time points and the reaction was stopped by adding one volume of ACN (50% ACN final concentration) and placing the reaction mixture on ice. IS was added and the extraction was performed as described in 2.3 and 2.4.

2.12. Animals experiments

The *in vivo* experiments with hemopressins and pepcan-23 were conducted using eight weeks old female CD-1 mice (25-30 g body weight) supplied by Janvier Laboratory. Mice were kept under standard environmental conditions (24 ± 2 °C; light-dark cycle of 12:12 h) with food and water *ad libitum*. Animals were handled according to Swiss federal legislation and guidelines of the local animal facility of the University of Bern. The protocols used (see below) were approved by the respective government authorities (Veterinäramt Kanton Bern, Switzerland) and operated under the license BE-79/18. Before starting the experiment, mice were habituated for one week.

2.13. In vivo distribution studies of hemopressin, RVD-hemopressin, and pepcan-23

Female CD-1 mice were injected intraperitoneally (i.p.) with the indicated peptides (100 mg/kg in saline, 50 μL). The mice were sacrificed by decapitation 15-60 min after i.p. administration. To quantify basal peptide levels, control group mice were i.p. injected with the vehicle and sacrificed. Brain, liver, kidney, spleen, adrenals, and trunk blood were collected for LC-MS/MS analyses. All tissues were briefly washed in ice-cold PBS, immediately snap-frozen in liquid nitrogen and stored at −80 °C until extraction. Blood sampled were collected in EDTA tubes and centrifuged to obtain plasma and the cellular fraction, stored at −80 °C until analysis.

2.14. Pepcan-23 degradation and RVD-hemopressin generation assay

The homogenates were prepared by homogenizing the tissue in ice-cold assay buffer (10 mM Tris-HCl pH 7.4) using a bead beater. The IRI tissue samples were used from previously published experiments. Samples were kept on ice until the experiment. Total protein concentration was determined using the BCA kit. Peptide (2 μM) was spiked into the homogenate (500 μg total protein/mL). The homogenate was incubated at 37 °C and 400 rpm in the thermoshaker. Aliquots of 200 μL were taken at the indicated time points and the reaction was stopped by adding one volume of ACN and placing the mixture on ice. IS was added to the sample and extraction was carried out as described in 2.3.

2.15. Pepcan-23 degradation in human whole blood homogenates

For the degradation experiments in whole blood homogenate, 4 μM pepcan-23 or RVD-hemopressin in water with or without 5 mM metal ion salt was prepared. Tested metal salts were either $CuCl_2$, $NiCl_2$, or a metal mixture containing $ZnCl_2$, $CaCl_2$, $MgCl_2$ and $MnCl_2$. Afterward, the same volume of whole blood homogenate (v/v) was added, and the reaction mixtures were incubated at 37 °C and extracted similar to 2.14. Homogenates were generated by mechanical disruption using a polytron homogenizer.

2.16. De novo and hierarchical structure prediction of pepcan-23

Prediction of the secondary structure and amphiphilicity of a α-helix of pepcan-23 was carried out using Chou-Fasman and GOR-I prediction (Garnier et al., 1978; Prevelige and Fasman, 1989). The structure of pepcan-23 was predicted using the *de novo* structure modeling software PepFold3, based on structural alphabet SA letters to describe the conformations of four consecutive residues and coupling the predicted series of SA letters to a greedy algorithm and a coarse-grained force field (Lamiable et al., 2016; Thévenet et al., 2012). Structure prediction was also performed using I-Tasser (Iterative Threading ASSEmbly Refinement), which identifies structural templates from the PDB by multiple threading approach LOMETS, with full-length atomic models constructed by iterative template-based fragment assembly simulations (Yang and Zhang, 2015; Zhang et al., 2017). PDB 2DN2 was used for the comparison of the pepcan-23 structure in the α-hemoglobin protein (Fig. 5C and E). Similar results were observed using PDB 1A3N, 4HHB, and 6BB5. For the data analysis and figure generation ChimeraX was used.

2.17. Statistical analysis

Statistical analyses were performed using GraphPad Prism 9. For the *in vivo* experiments, the analysis from peptide injected mice versus the vehicle treated control group was performed using Kruskal-Wallis test followed by Dunn's post-hoc analysis. Other statistical analyses are indicated in the figure legends of the corresponding experiments. Where appropriate, SEM (standard error of the mean) or SD (standard deviation) were shown.

3. Results

3.1. Quantification method of hemopressins and pepcan-23 using LC-MS/MS

Using optimized protein precipitation and SPE enabled us to selectively and sensitively extract and quantify the peptides hemopressin (PVNFKLLSH), RVD-hemopressin (RVDPVNFKLLSH) and pepcan-23 (SALSDLHAHKLRVDPVNFKLLSH). The C8 column was the most efficient for the LC separation of these peptides spanning a broad range of sizes (1054 Da–2598 Da) (Supplementary Fig. 1). With the established LC-MS/MS method (Table 1), the peptides could be detected as low as 0.2 ng/mL and they were quantified with an accuracy $\geq$ 85% throughout the concentration range 0.4–10000 ng/mL. MRM parameters are shown in Supplementary Table 1.

Calibration curves were always freshly prepared because of the low stability of the peptides in solution upon freeze and thaw cycles

Table 1
Quantification of the different peptides. MRM transitions, limit of detection (LOD) and range of quantification are shown.

Peptide	MRM transition	LOD	Quantifiable range
Hemopressin	352.7/120.0	0.2 ng/mL	0.4–10000 ng/mL
RVD-hemopressin	475.7/371.1	0.2 ng/mL	0.5–10000 ng/mL
Pepcan-23	520.5/131.0	0.2 ng/mL	0.6–10000 ng/mL

(Supplementary Table 2). Method validation (recovery, stability, and matrix effects) and parameters are reported the method section and Supplementary Tables 2–5. Recovery of the QCs of all peptides ranged from 45 to 90% (Supplementary Table 3). The peptides exhibited no carry over in the measurements. In the autosampler they were stable (>90%) for at least three days (Supplementary Table 4). However, peptides spiked into neat solution (without any matrix or extraction procedure), resulted in a significant loss of signals. As soon as a matrix (e.g., diluted tissues or 0.1% BSA solution) was introduced in any step of the procedure, the signals remained constant, and five-fold higher compared to neat solution indicating a strong matrix effect. The intra-assay coefficient of variation of the three-quality control (QC) samples ranged from 2 to 38% and the inter -assay coefficients of variation of three independent calibration curves ranged between 7 and 35% (Supplementary Table 5). In human whole blood, RVD-hemopressin and pepcan-23 were found at 143 ± 89 pmol/mL and 57 ± 47 pmol/mL, respectively. Interestingly, pepcan-23 and RVD-hemopressin were mostly present in the cellular fraction and only traces (3-10% of total) could be found in plasma or serum. As previously reported, hemopressin was not present when using the neutral extraction method but was readily generated from RVD-hemopressin and possibly pepcan-23 as an artifact when using acidic pH extraction protocols, approximately equaling the total amounts of RVD-hemopressin (Fig. 1).

3.2. Stability of hemopressins and pepcan-23 in whole blood, plasma and serum

To assess the impact of peptide length and structure on pharmacokinetic parameters, the metabolic stability of hemopressin, RVD-hemopressin and pepcan-23 was measured in independently spiked blood tissue matrices of varying complexity. As seen in Fig. 2, pepcan-23 was the most stable peptide in all blood matrices *ex vivo*. After 5 min incubation in human whole blood, pepcan-23 remained fully stable, but RVD-hemopressin and hemopressin were already degraded by approximately 20%. After 15 min, approximately 50% of hemopressin and RVD-hemopressin were degraded. Conversely, pepcan-23 was significantly more stable over 30–45 min. After 2 h in whole blood pepcan-23 was degraded by approximately 70% and hemopressin and RVD-hemopressin were almost fully degraded. Interestingly, pepcan-23 partially (3-10%) converted into RVD-hemopressin, depending on the blood donor. In serum and plasma, pepcan-23 remained fully stable over 2 h, whereas RVD-hemopressin and hemopressin were degraded time-dependently in all conditions (Fig. 2). Despite the fact that RVD-hemopressin was present endogenously in blood (associated to the cellular fraction) and in some donors at higher amounts than pepcan-23 (Fig. 1B), *ex vivo* incubation of RVD-hemopressin showed the lowest stability in plasma, serum and whole blood (Fig. 2).

3.3. Bioavailability and tissue distribution of hemopressins in mice

Considering the apparent differences observed in the *ex vivo* stability studies of hemopressin, RVD-hemopressin and pepcan-23 (Fig. 2), we next investigated the bioavailability/metabolic stability and tissue distribution of these peptides in CD-1 mice upon intraperitoneal (i.p.) administration (100 mg/kg in saline). The animals were sacrificed at different time-points (15-60 min). Rather unexpectedly, hemopressin was not detected at all in any of the tissues and already after 15 min the amounts were below the limit of quantification, strongly indicating that this nonapeptide is degraded rapidly *in vivo* (Supplementary Fig. 2). On the other hand, RVD-hemopressin was somewhat more metabolically stable than hemopressin and significantly increased in spleen at 20 and 60 min after

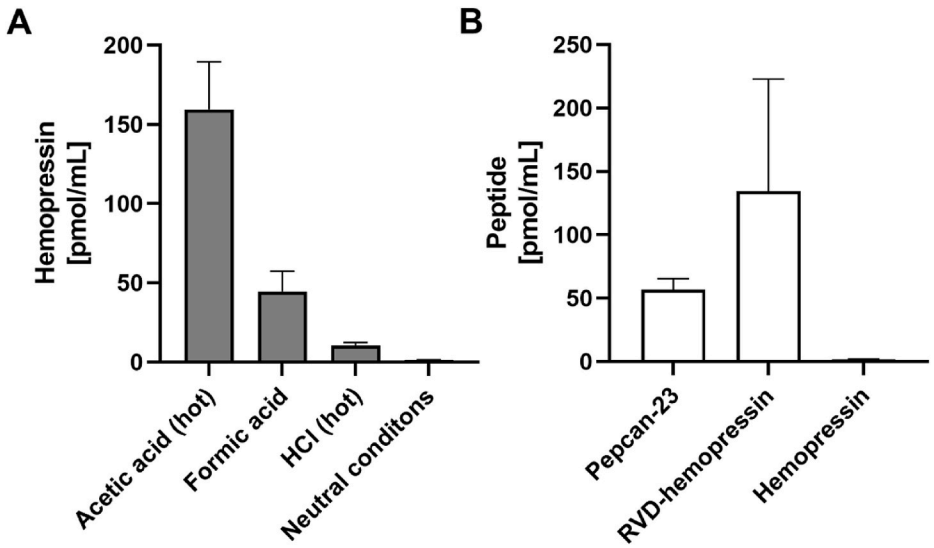

Fig. 1. Extraction of hemopressin, RVD-hemopressin and pepcan-23 from human whole blood. (**A**) Under different acidic conditions (pH < 3) significant amounts of hemopressin were generated (n ≥ 3) (**B**) Extraction and quantification of peptides under neutral (pH 7) conditions (n ≥ 20). Data show mean values ± SD of three independent experiments from human whole blood samples pooled of at least three different donors.

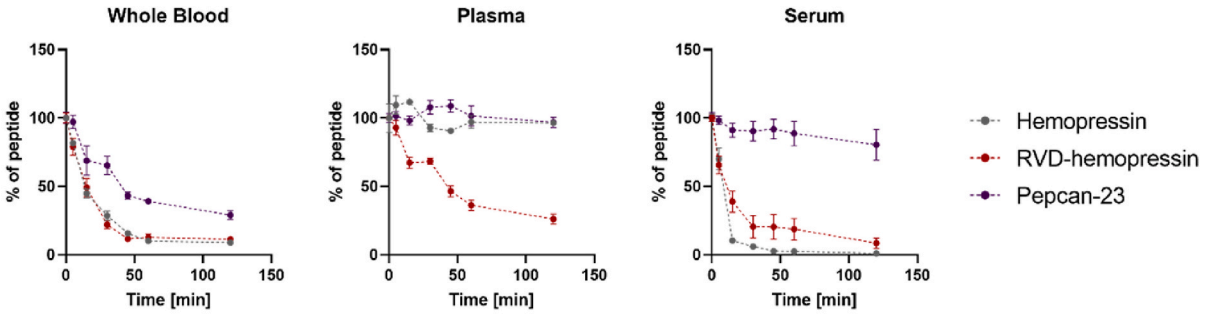

Time [min]		0	5	15	30	45	60	120
Hemopressin [%]	Whole blood	100.0 ± 3.2	81.7 ± 3.3	44.9 ± 5.7	28.7 ± 5.8	15.9 ± 2.4	10.2 ± 1.2	9.0 ± 1.4
	Plasma	100.0 ± 18.0	109.5 ± 11.6	111.8 ± 2.3	92.9 ± 4.6	90.7 ± 2.6	97.2 ± 8.0	96.5 ± 1.3
	Serum	100.0 ± 6.5	70.1 ± 19.3	10.4 ± 0.8	6.0 ± 1.6	2.8 ± 1.1	2.5 ± 0.5	1.0 ± 0.2
RVD-hemopressin [%]	Whole blood	100.0 ± 8.7	79.1 ± 15.2	49.2 ± 16.1	22.0 ± 7.2	11.7 ± 5.1	12.8 ± 3.9	11.4 ± 2.1
	Plasma	100.0 ± 5.0	92.9 ± 13.4	67.3 ± 8.8	68.3 ± 4.0	46.6 ± 9.7	36.4 ± 9.7	26.2 ± 8.9
	Serum	100.0 ± 9.5	65.7 ± 27.6	39.0 ± 26.6	20.6 ± 20.0	20.5 ± 22.2	18.8 ± 19.4	8.5 ± 11.3
Pepcan-23 [%]	Whole blood	100.0 ± 9.8	97.2 ± 11.8	76.6 ± 19.1	65.6 ± 16.2	43.4 ± 4.5	39.1 ± 3.4	29.0 ± 5.5
	Plasma	100.0 ± 8.0	101.4 ± 8.1	98.2 ± 8.0	108.0 ± 12.4	108.9 ± 1.3	101.6 ± 17.8	97.0 ± 9.1
	Serum	100.6 ± 10.9	87.9 ± 26.5	91.1 ± 16.4	90.4 ± 21.6	92.0 ± 21.3	88.9 ± 22.0	54.2 ± 44.9

Fig. 2. Metabolic stability of peptides in human whole blood, plasma and serum. The stability of hemopressin, RVD-hemopressin and pepcan-23 was measured independently in human whole blood, human plasma, and human serum at 37 °C. The starting time point (0 min, 100%) represents the maximum spiked amount (2 μM) at the beginning of each experiment. Data show mean values ± SD of at least three independent experiments, each performed in triplicates, from blood of 3–10 human donors. The remaining percentage of each peptide at the indicated time points is summarized in the table below.

injection (Supplementary Fig. 3). Upon RVD-hemopressin injection, in most tissues no increase above basal levels could be measured (Supplementary Fig. 3). A trend towards increased RVD-hemopressin tissue levels were found at 20 min in liver and kidney (Supplementary Fig. 3). Importantly, we did not find evidence that RVD-hemopressin crossed the blood-brain barrier and accumulated in the brain.

3.4. Metabolic stability of pepcan-23 and conversion to RVD-hemopressin (pepcan-12) in vivo

When pepcan-23 (100 mg/kg) was injected intraperitoneally in mice we observed that not only the amounts of pepcan-23 accumulated in different tissues, but also the amounts of RVD-hemopressin increased simultaneously (Fig. 3).

Due to its superior stability over the shorter hemopressins, pepcan-23 was found in plasma 15 min after injection and remained quantifiable for 30 min (Fig. 3). Pepcan-23 levels returned to basal levels 60 min after injection (some tissue levels were <LOQ). In liver, spleen, and kidney pepcan-23 levels were increased 15 min after i.p. injection and RVD-hemopressin levels were increased simultaneously in these tissues 15 min after i.p. injection of pepcan-23, showing *de novo* generation of this peptide most likely resulting from the specific cleavage of its pro-peptide pepcan-23. A tendency towards increased pepcan-23 and RVD-hemopressin in the brain was measured (Supplementary Fig. 4).

3.5. RVD-hemopressin production from pepcan-23 in adrenal gland and liver homogenates

We next analyzed the conversion of pepcan-23 to RVD-hemopressin in adrenal gland and liver homogenates. As shown in Fig. 4A, upon spiking of pepcan-23 into adrenal homogenates RVD-hemopressin increased significantly after 10 min and the amounts of pepcan-23 and RVD-hemopressin correlated inversely. Since the homogenate contained numerous non-specific proteases and peptidases, only approximately 5% of the conversion could be observed. In a previous study we have found that not only adrenals are important for the production and storage for pepcans, but also the levels of both pepcan-23 and RVD-hemopressin were increased in liver tissues coming from a mouse model of IRI (Petrucci et al., 2017). Additionally, RVD-hemopressin and pepcan-23 levels were dramatically decreased in all tissues after adrenalectomy, in line with the finding that noradrenergic cells express pepcans/hemopressins. We thus spiked pepcan-23 into liver homogenates of wild-type (wt) and adrenalectomized mice suffering from IRI. As shown in Fig. 4B, pepcan-23 was degraded in all three liver homogenates with similar kinetics. In the IRI liver homogenate of both wt

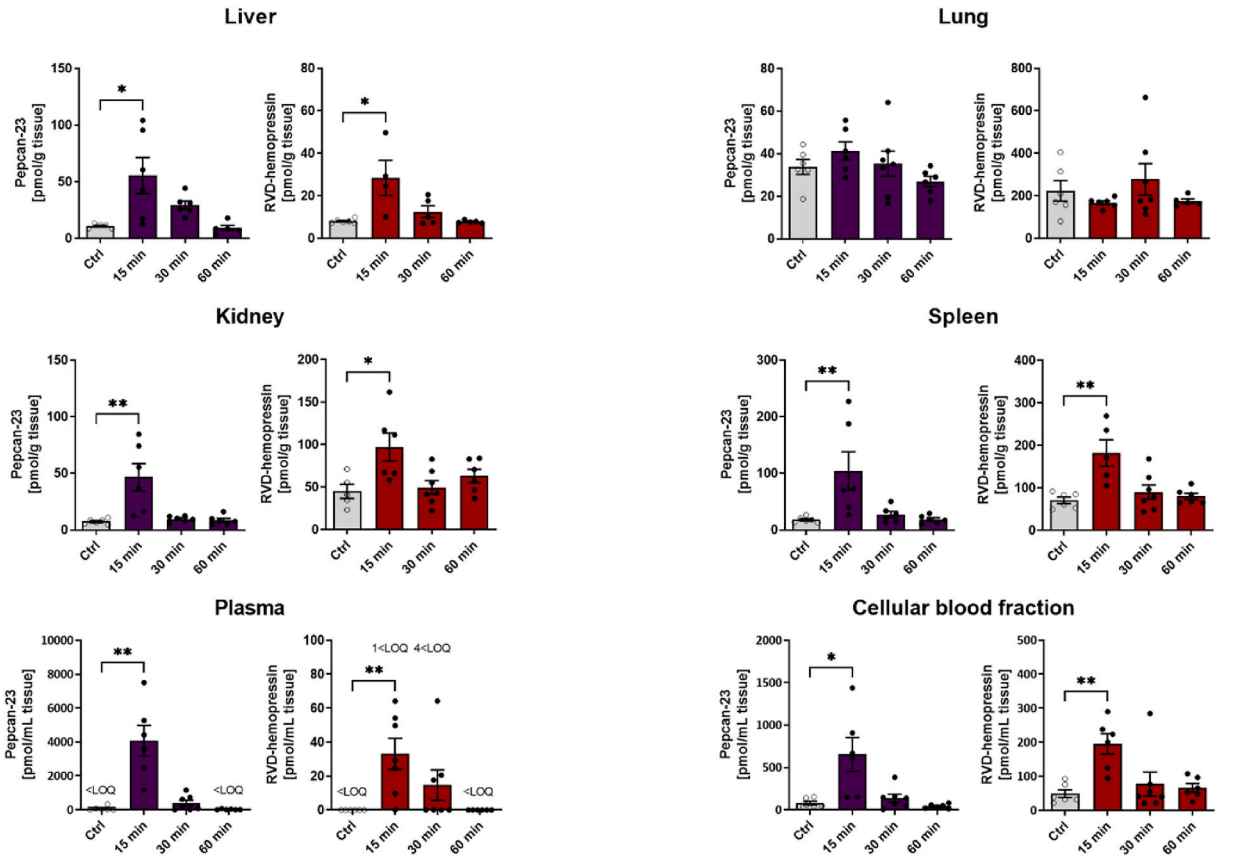

Fig. 3. Pepcan-23 accumulates in tissues and is converted to RVD-hemopressin *in vivo*. Pepcan-23 (100 mg/kg in saline) was injected i.p. to CD-1 mice (female, 8 weeks old) and pepcan-23 and RVD-hemopressin were extracted and quantified by LC-MS/MS at indicated time points. The amounts of pepcan-23 (purple) and RVD-hemopressin (red) are shown. Data show mean values ± SEM. Each dot represents the measured value of one animal. Data were analyzed and compared to control group (Ctrl, saline group) using Kruskal-Wallis test followed by Dunn's post-hoc analysis. *, $p < 0.05$, **, $p < 0.01$ compared to saline group. n = 6–7. Limit of quantification = LOQ, n.d. = not detected.

and adrenalectomized mice significantly more RVD-hemopressin was generated (20x compared to baseline) (Fig. 4B).

3.6. Acute administration of hemopressin in mice and its impact on RVD-hemopressin, pepcan-23 and the endocannabinoid lipidome

In light of the previous studies reporting pharmacological effects upon i.p. administration of hemopressin (Supplementary Table 6), as well as the shared peptide sequence with endogenous RVD-hemopressin and pepcan-23, we hypothesized that hemopressin may modulate the degradation of these peptides or could impact eCB levels. Upon single hemopressin administration (100 mg/kg), we observed a tendency towards increased corticosterone levels, possibly due to the xenobiotic stress of the high peptide load. Intriguingly, hemopressin could not be detected in any of the tissues at any of the time points (15, 30 and 60 min), indicating that hemopressin is rapidly degraded *in vivo*. No significant time-dependent effects on the endogenous levels of RVD-hemopressin or pepcan-23 were measured in any tissue (Supplementary Fig. 2). In the kidney and liver there was a tendency towards reduced pepcan-23 levels. Neither AEA nor the N-acylethanolamines were significantly modulated (Supplementary Figs. 5–11). However, 15 min post hemopressin injection, 2-AG levels were reduced in the lung by approximately 50%. This reduction was not seen in the group 30 min post hemopressin injection. Interestingly, we observed an increase of 1-stearoyl-2-arachidonoyl-sn-glycerol (SAG) in plasma at the later time points and a clear tendency towards increased SAG and 2-AG in brain (Supplementary Figs. 5 and 6).

3.7. Conformational analysis of pepcan-23 by CD spectroscopy

Given the distinct metabolic fates of hemopressins and pepcan-23 *ex vivo* and *in vivo*, we addressed the differences related to the secondary structure of these peptides in physiological conditions. The conformational properties of pepcan-23, RVD-hemopressin and hemopressin were analyzed in aqueous solution (PB buffer, 10 mM) at different pH (pH 4.5–9) employing CD spectroscopy. The CD spectra were compared to the secondary structure of pepcan-23 in the α-hemoglobin chain (Fig. 5) as well as *in silico* employing *de novo* peptide structure 3D prediction software PEP-FOLD3 and the hierarchical approach of I-Tasser (Fig. 5 and Supplementary Fig. 12). The

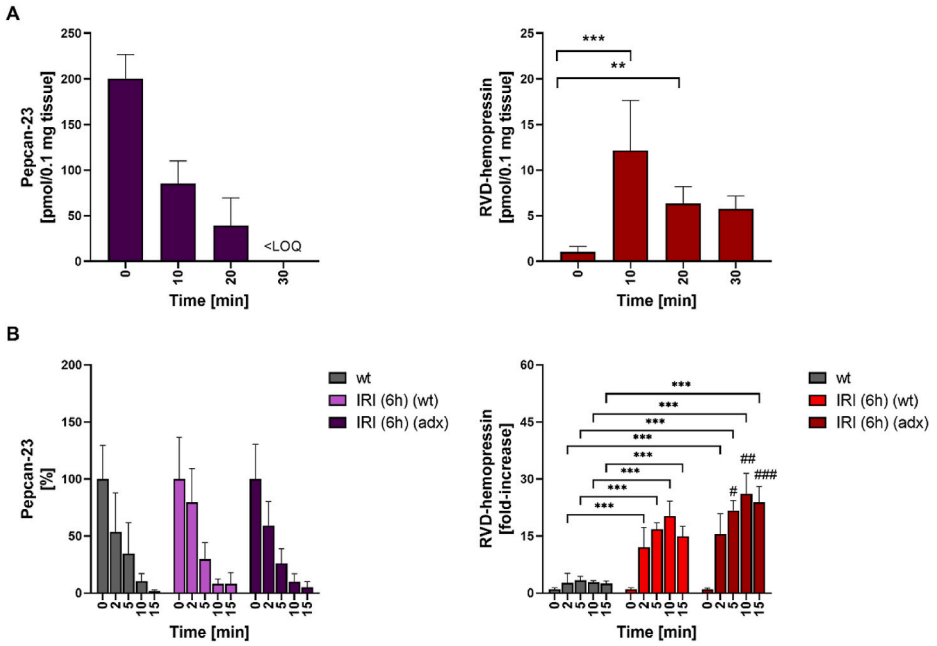

Fig. 4. Generation of RVD-hemopressin from pepcan-23 in adrenal gland and liver homogenates measured by LC-MS/MS. (**A**) Pepcan-23 (1 μM) was spiked into adrenal gland homogenates (1 mg/mL protein) showing a time-dependent degradation of pepcan-23 and simultaneous formation of RVD-hemopressin. (**B**) Pepcan-23 (2 μM) was spiked into liver homogenates (0.5 mg/mL protein) from healthy and ischemia reperfusion injury (IRI) mice with adrenalectomy (adx) and sham operated (wt) showing a time-dependent degradation of pepcan-23 and simultaneous formation of RVD-hemopressin. Data show mean values ± SD from at least three independent experiments, each performed in triplicates. Statistical analysis compared to 0 min, A Kruskal-Wallis test and Dunn's post hoc test *, $p < 0.05$, **, $p < 0.01$ ***, $p < 0.001$. B two-way ANOVA followed by Turkey's multiple comparison. *, $p < 0.05$, **, $p < 0.01$ ***, $p < 0.001$. Comparison wt IRI versus adx IRI 6 h, #, $p < 0.05$, ##, $p < 0.01$ ###, $p < 0.001$.

secondary structures of the nonapeptide hemopressin and RVD-hemopressin could not be predicted accurately *in silico* as the software only allowed meaningful predictions of peptide sequences >20 amino acids. As summarized in Table 2, pepcan-23 contains amino acids flanking proline which prefer to form α-helices or turns as secondary structure. This was also calculated by *de novo* structure prediction (Fig. 5A–C).

The amino acid sequence of pepcan-23 and RVD-hemopressin, respectively, is exclusively present in α-hemoglobin. The structure of hemoglobin (human, adult hemoglobin, PDB 6KYE) was therefore extracted to visualize the conformation of the pepcan-23 (SALSDLHAHKLRVDPVNFKLLSH) in the α-hemoglobin chain (Fig. 5D). In the protein, pepcan-23 consists of two right-turning α-helices (SALSDLHAHK and PVNFKLLSH), connected by an unordered part (LRVD). One α-helix corresponded to the hemopressin sequence PVNFKLLSH (Fig. 5B) and the other α-helix to the N-terminal part of pepcan-23. The kink caused by proline in the α-helix acting as "structure breaker" is well visible (Fig. 5E). The C-terminal α-helix of the hemopressin sequence stops precisely at that point, leading to the unordered part of the sequence.

The CD spectra were also recorded at different pH in PB buffer (Supplementary Fig. 13). The results suggested that the structure of pepcan-23 is mostly disordered. Deconvolution of pepcan-23 indicated up to 30% α-helical content and 8% β-sheet content at physiological pH (7.4) (Supplementary Fig. 13). Comparing the structural content of pepcan-23 to the shorter peptides hemopressin and RVD-hemopressin, deconvolution indicated that the longer peptide was more structured than the shorter ones. To analyze conformational changes that may occur at physiological pH in less polar environments, for example as it would be the case at a specific receptor binding site at the plasma membrane, we used solvent mixtures containing 0–100% of TFE at physiological pH 7.4 (Fig. 6). TFE has been widely used as a versatile structure inducing co-solvent for NMR and CD studies because it promotes intra-peptide interactions over peptide-solvent interactions. TFE can induce the formation of stable conformations in peptides (α-helix, β-sheet) which are otherwise unstructured in aqueous solution (Roccatano et al., 2002; Sönnichsen et al., 1992; Tamburro et al., 1968). Not unexpectedly, our data show that TFE clearly increased the α-helical content in all three peptides (Fig. 6, Table 3).

In PB buffer without TFE, pepcan-23 exhibited the highest α-helical content (12.5%) as compared to hemopressin (10.8%) and RVD-hemopressin (6.6%). Hemopressin exhibited an increased α-helical content at >30% TFE. RVD-hemopressin and pepcan-23 already at 5% TFE showed an increased α-helical content and the maximal α-helical content was reached for all three peptides at 100% TFE (hemopressin: 18%, RVD-hemopressin: 27% and pepcan-23: 44%) (Fig. 6B). However, the lower TFE buffer mixtures mimic more closely a biological environment as 100% is artificially forcing peptide conformational changes (Arunkumar et al., 1997). Nonetheless, pepcan-23 underwent significant conformational changes already at 5-20% TFE, decreasing the β-sheet and increasing the α-helical conformation content, respectively (Table 3, Fig. 6B). Conversely, hemopressin had the highest β-sheet content among the

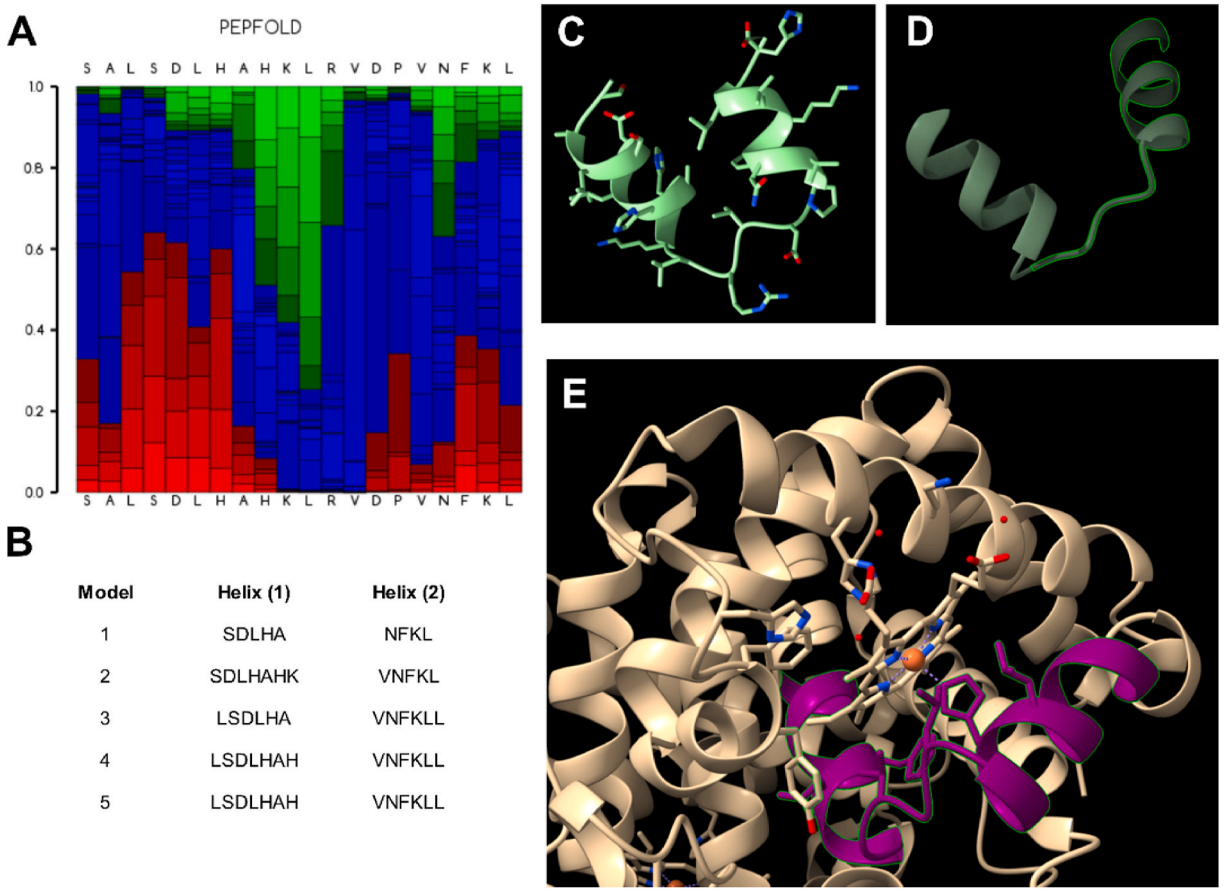

Model	Helix (1)	Helix (2)
1	SDLHA	NFKL
2	SDLHAHK	VNFKL
3	LSDLHA	VNFKLL
4	LSDLHAH	VNFKLL
5	LSDLHAH	VNFKLL

Fig. 5. ***De novo*** **structure prediction of pepcan-23 and conformation of the pepcan-23 sequence SALSDLHAHKLRVDPVNFKLLSH in the α-hemoglobin chain.** (**A**) Graphical representation of the probabilities of each Structural Alphabet (SA) letter at each position of the entered sequence using the *de novo* structure modeling software Pep-FOLD3. Each SA letter corresponds to fragments of 4 residue length. The heat map shows the predicted local structure of the pepcan-23 (red: helical, green: extended, blue: coil). (**B**) Structural composition of the two helices in five different models obtained by PEP-FOLD3. (**C**) Representative models of pepcan-23 showing two helices connected by an unordered part obtained using Pep-FOLD3. (**D**) Isolated secondary structure of pepcan-23 in the human α-hemoglobin protein. Image was visualized using the ChimeraX software. (**E**) Pepcan-23 coordinates the Fe(II) binding in the α-hemoglobin structure. The pepcan-23 sequence is highlighted in violet. Image was generated using the ChimeraX software.

Table 2
Secondary structure prediction of pepcan-23. Prediction of the secondary structure and amphiphilic helix of pepcan-23 (for reference see methods 2.16).

Amphiphilic Helix	SALSDLHAHKLRVDPVNFKLLSH	Helix
Secondary Structure Prediction	SALSDLHAHKLRVDPVNFKLLSH SALSDLHAHKLRVDPVNFKLLSH	Turn, Beta Alpha

tested peptides in all TFE conditions at pH 7.4. RVD-hemopressin initially revealed a β-sheet content of approximately 30%, which was slightly decreasing (to 25%) with increasing amounts of TFE. In contrast, pepcan-23 had the lowest content of β-sheets (27%) which significantly reduced upon TFE addition (5-10%) while the helical content was increasing (44%) (Fig. 6C, Table 3). Fig. 6C shows the relation of the distinct conformational changes of hemopressin, RVD-hemopressin and pepcan-23 as a function of TFE content in the PB buffer. For all peptides, the unordered conformational content remained constant at all TFE concentrations (Supplementary Fig. 14).

3.8. CD spectroscopy of hemopressins and pepcan-23 upon metal ion binding

It was previously reported that hemopressin and RVD-hemopressin bind Cu(II) and Ni(II) at basic but not at acidic pH (Remelli et al., 2016). For comparison, in addition to physiological pH we also tested these peptides as well as pepcan-23 at pH 9 and pH 4.5. Generally, Cu(II) ions exhibit a high affinity towards nitrogen donors and are among the few metal ions able to deprotonate and

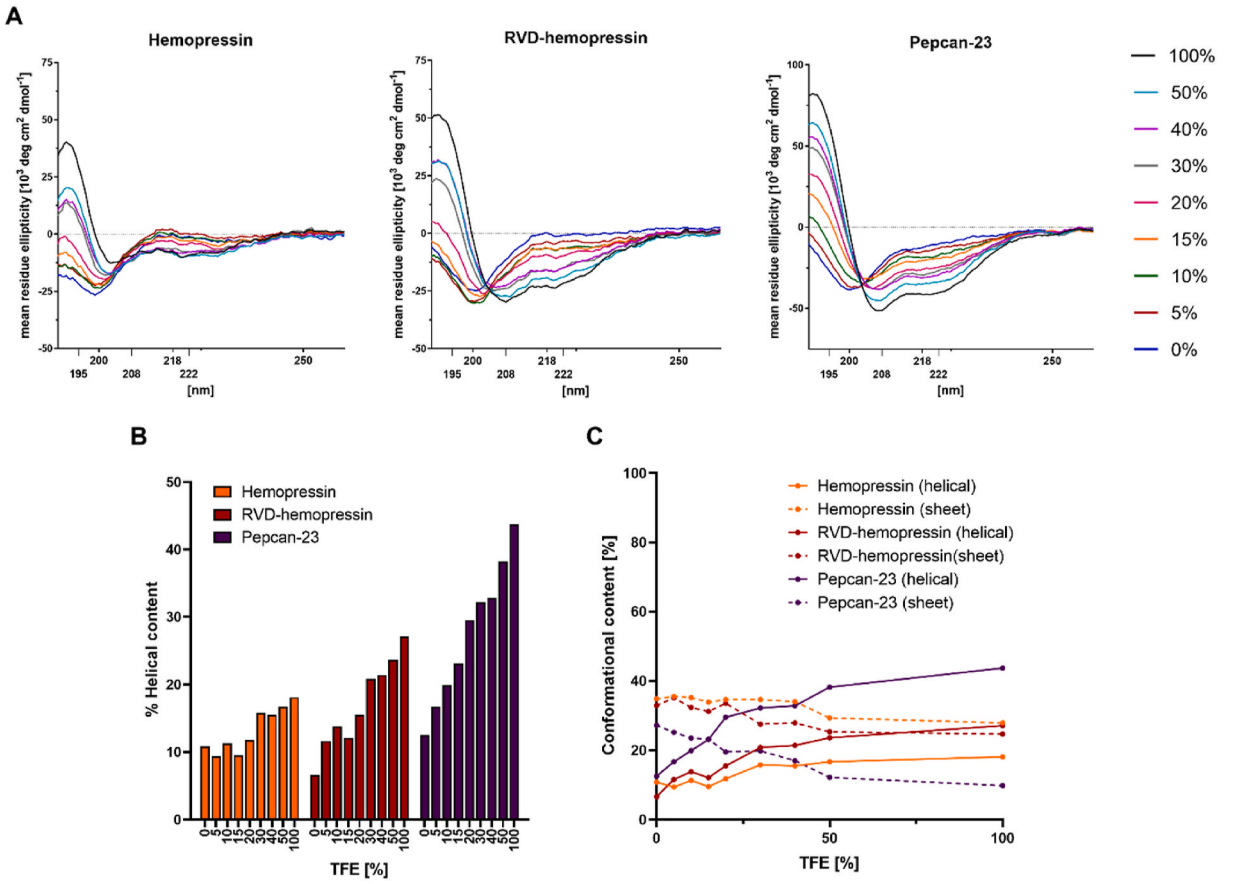

Fig. 6. CD spectra of conformational changes induced by TFE. (**A**) CD spectra of hemopressin, RVD-hemopressin and pepcan-23 (200 μg/mL) in TFE solution (0-100%) at pH 7.4 in 10 mM phosphate buffer (PB). (**B**) The calculated percentage of the α-helical content at different concentration of TFE. (**C**) Percentage of α-helical and β-sheet content as a function of the concentration of TFE. Data were processed by Dichroweb using the CONTIN LL analysis and reference set 3.

Table 3
TFE induced changes in conformational properties measured by CD spectroscopy. Data were processed by Dichroweb using the CONTIN LL analysis and reference set 3.

	TFE [%]	0	5	10	15	20	30	40	50	100
Hemopressin	α-helix [%]	10.8	9.4	11.3	9.5	11.8	15.8	15.5	16.7	18.1
	β-sheet [%]	34.8	35.5	35.2	33.9	34.6	34.6	34.0	29.3	27.9
	Unordered [%]	32.7	33.0	32.4	33.8	32.6	32.7	31.0	31.2	30.6
RVD-hemopressin	α-helix [%]	6.6	11.6	13.8	12.1	15.5	20.8	21.4	23.6	27.1
	β-sheet [%]	32.9	35.1	32.3	31.2	33.5	27.5	27.9	25.3	24.7
	Unordered [%]	34.2	33.2	32.9	32.9	31.4	30.1	28.5	28.7	27.1
Pepcan-23	α-helix [%]	12.5	16.7	19.9	23.1	29.5	32.2	32.8	38.2	43.7
	β-sheet [%]	27.2	25.2	23.5	23.2	19.5	19.8	17	12.2	9.8
	Unordered [%]	34.0	32.7	31.8	30.4	27.7	26.3	27.2	25.6	23.6

coordinate a peptide bond nitrogen (Gonzalez et al., 2018). Hemopressin was reported to show conformational changes upon Cu(II) binding at pH 7.5 or higher. Given the higher α-helical content in pepcan-23 we examined whether pepcan-23 could bind Cu(II) and Ni (II) ions at physiological conditions (pH 7.4). In agreement with the previous data (Remelli et al., 2016), hemopressin and RVD-hemopressin bound Cu(II) at pH 7.4 and pH 9, but not at pH 4.5 (Fig. 7B and C). As shown in Fig. 7, the conformational changes were visible by comparing peptides co-incubated with metals (blue or green dashed lines) with peptides in buffer only (grey line). For pepcan-23, which was analyzed for the first time, similar conformational changes could be observed at pH 7.4 and pH 9 upon incubation with Cu(II) and Ni(II), but not at acidic pH. In the CD spectroscopy experiments, the effect of pepcan-23 Cu(II) interaction was more substantial compared to Ni(II), but overall pepcan-23 performed similarly to hemopressin and RVD-hemopressin.

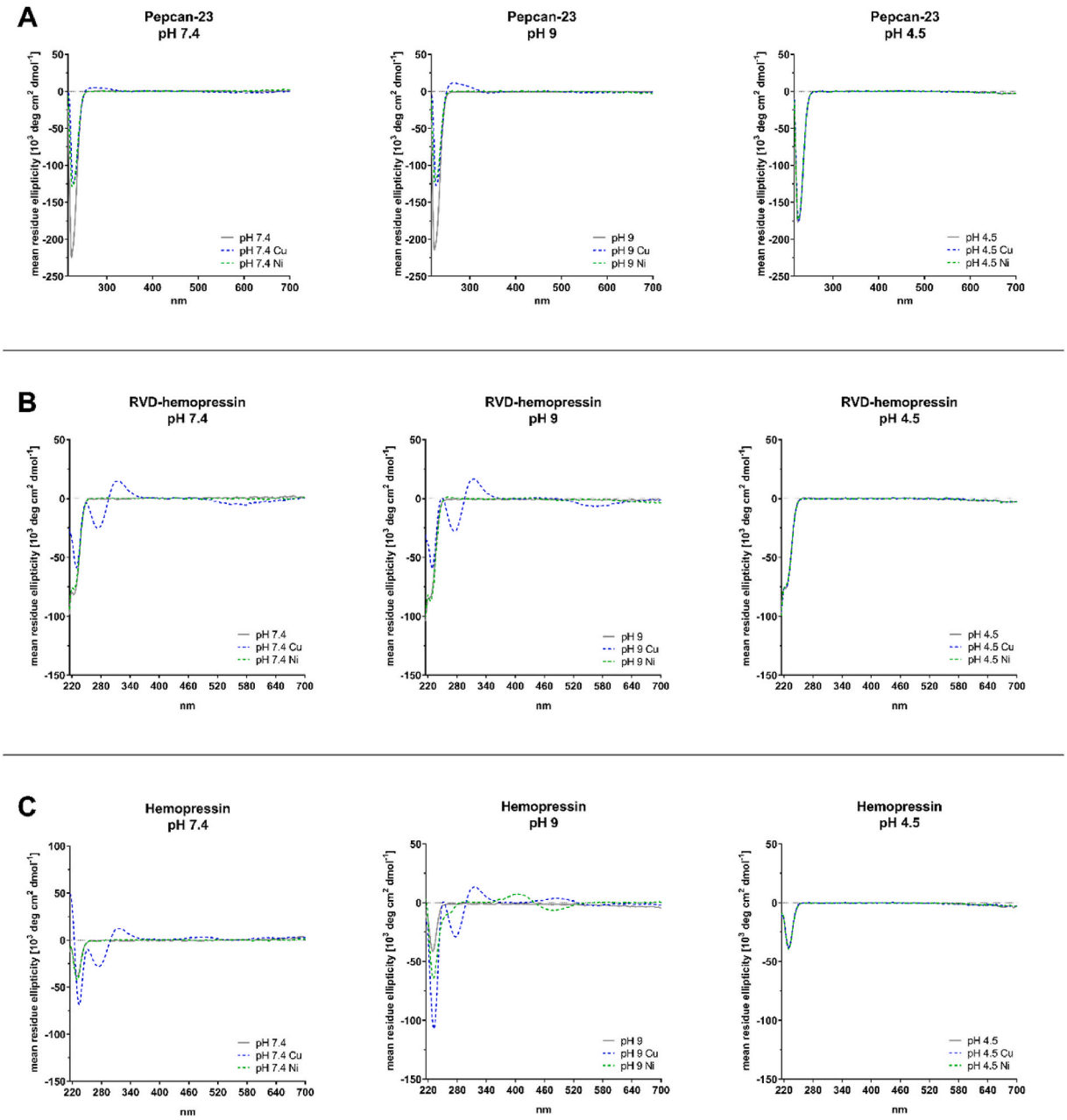

Fig. 7. CD spectra of hemopressins and pepcan-23 in presence of Cu(II) and Ni(II). CD spectra of (**A**) pepcan-23, (**B**) RVD-hemopressin and (**C**) hemopressin were recorded at different pH (pH 4.5, pH 7.4, pH 9) in absence or presence of Cu(II) and Ni(II). The peptides interact with Cu(II) and Ni(II), especially at pH 7.4 and pH 9 as the conformational changes indicate. No interaction with metals is observed at pH 4.5. Temperature 25 °C, 1.1 mM peptide, 1 mM $NiCl_2$ or $CuCl_2$.

3.9. ESI-MS analyses on pepcan-23 metal ion adducts

To confirm the pepcan-23 metal interactions observed in CD spectroscopy, we performed ESI-MS experiments. The ESI-MS experiments showed that pepcan-23 binds Cu(II) and Ni(II) (Fig. 8, Supplementary Figs. 15–17, Supplementary Table 7). Different molar ratios of peptide and metals were tested (1:1, 1:2 and 1:10). At a ratio of 1:1, the Cu(II)-pepcan-23 adduct appeared in the spectrum at m/z 1331.3 (2+), 887.9 (3+), 666.8 (4+), 533.5 (5+) and 444.7 (6+) (Supplementary Table 7, Supplementary Fig. 17). With increasing amounts of Cu(II) (1:2 and 1:10 ratio), m/z values containing up to three copper atoms could be found (Fig. 8, Supplementary Fig. 15). For comparison, the spectrum of pepcan-23 in the absence of metal ions and an overlapping spectrum of pepcan-23 and pepcan-23:Cu(II) (1:10 ratio) are shown in Supplementary Fig. 16. As in the case of copper, up to three nickel atoms could bind to

A

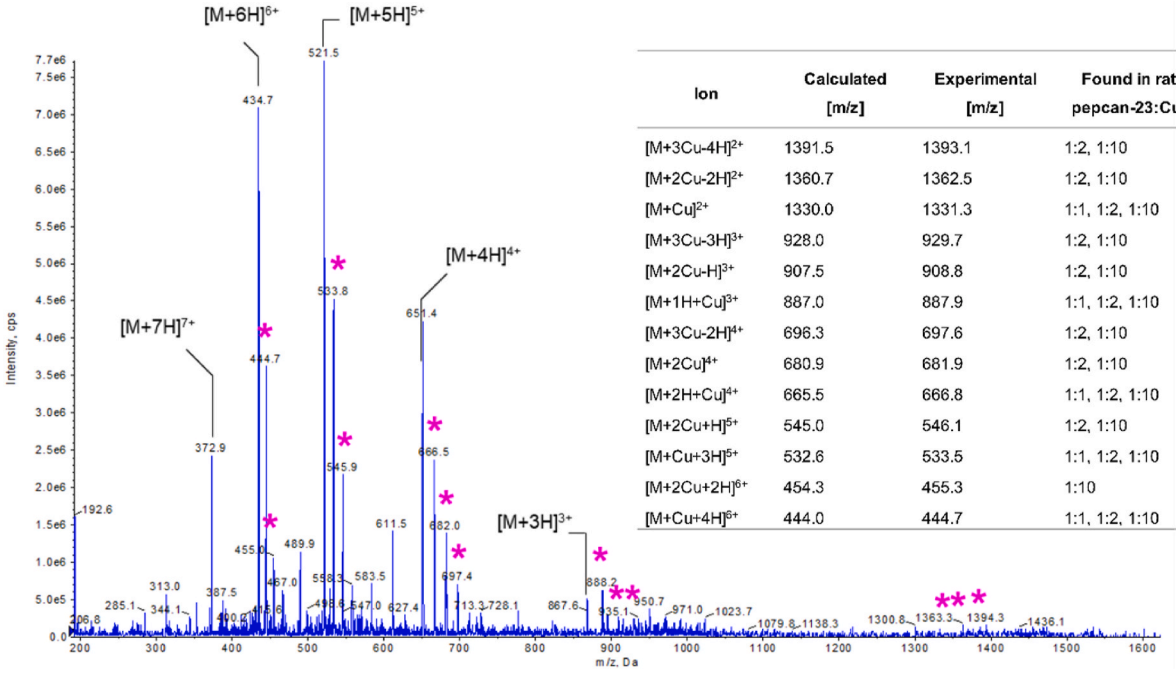

B

Ion	Calculated [m/z]	Experimental [m/z]	Found in ratio pepcan-23:Cu(II)
$[M+3Cu-4H]^{2+}$	1391.5	1393.1	1:2, 1:10
$[M+2Cu-2H]^{2+}$	1360.7	1362.5	1:2, 1:10
$[M+Cu]^{2+}$	1330.0	1331.3	1:1, 1:2, 1:10
$[M+3Cu-3H]^{3+}$	928.0	929.7	1:2, 1:10
$[M+2Cu-H]^{3+}$	907.5	908.8	1:2, 1:10
$[M+1H+Cu]^{3+}$	887.0	887.9	1:1, 1:2, 1:10
$[M+3Cu-2H]^{4+}$	696.3	697.6	1:2, 1:10
$[M+2Cu]^{4+}$	680.9	681.9	1:2, 1:10
$[M+2H+Cu]^{4+}$	665.5	666.8	1:1, 1:2, 1:10
$[M+2Cu+H]^{5+}$	545.0	546.1	1:2, 1:10
$[M+Cu+3H]^{5+}$	532.6	533.5	1:1, 1:2, 1:10
$[M+2Cu+2H]^{6+}$	454.3	455.3	1:10
$[M+Cu+4H]^{6+}$	444.0	444.7	1:1, 1:2, 1:10

Fig. 8. ESI-MS spectrum of pepcan-23 Cu(II) adducts. Pepcan-23 was incubated with Cu(II) in solution. (**A**) Spectrum indicating the molecular peaks of pepcan-23 and showing the formed Cu(II) adducts (pink asterix). At a molar ratio 1:10 of pepcan-23 to Cu(II) mostly adducts with two or three Cu(II) ions are formed. In the spectrum, peaks corresponding to one Cu(II) bound to pepcan-23 are still visible but to a significantly lower intensity. Molar ratio (1:10) of pepcan-23 to Cu(II) (0.6 mM peptide used). (**B**) List of ions, m/z values and used ratio peptide:Cu(II) the indicated ion was found.

pepcan-23 with an increasing ratio of peptide to metal (Supplementary Fig. 17). For copper and nickel, the metal peptide stoichiometry suggests a peptide complex with one to three metal ions (Fig. 8, Supplementary Figs. 15–17, Supplementary Table 7).

3.10. Pepcan-23 metal-binding regulates conversion to RVD-hemopressin and increases metabolic stability

Considering the superior metal-binding properties of pepcan-23 compared to hemopressins we were interested in the physiological implications of the pepcan-23 metal complex. To that aim, we measured the metabolic stability of pepcan-23 in the absence and presence of $CuCl_2$ and $NiCl_2$. As shown in Fig. 9A, preincubation with either $CuCl_2$ or $NiCl_2$ had a significant effect on pepcan-23 conversion to RVD-hemopressin in human whole blood homogenate. We also assessed the impact of other divalent metals ($ZnCl_2$, $CaCl_2$, $MgCl_2$, $MnCl_2$) as mixture on peptide metabolic stability. As shown in Fig. 9A, pepcan-23 was degraded over time and rather strikingly, this degradation was fully inhibited by preincubation of the peptide with the divalent metals (Cu(II), Ni(II), or metal mixture). On the other hand, preincubation with the same metal mix or Cu(II) or Ni(II) did not fully prevent the degradation of RVD-hemopressin (Fig. 9B).

4. Discussion

Despite the relatively recent description of hemopressin/pepcans, there is an increasing interest in hemopressin-type peptides as potential novel modulators of the ECS (Heimann et al., 2021). However, the elucidation of the biological roles of hemopressins as endogenous modulators of CB receptors have been convoluted by contradictory pharmacological results and, above all, the lack of analytical studies of these peptides *in vivo* (*vide infra*). In 2003, Rioli et al. have isolated and sequenced different peptides as hemoglobin fragments by ESI tandem mass spectrometry. Among them, the nonapeptide PVNFKFLSH, matching an α-hemoglobin fragment, was identified and named hemopressin (Rioli et al., 2003). In 2007, Heimann et al. showed that this nonapeptide interacted with CB1 receptors and behaved as an inverse agonist/antagonist *in vitro* (Heimann et al., 2007). Subsequently, Gomes et al. identified a three amino acid longer peptide and named it RVD-hemopressin in mouse brain extracts, but quite unexpectedly characterized this endogenous peptide as an agonist at CB1 receptors, mainly based on Gq signaling effects *in vitro* (Gomes et al, 2009, 2010). However, the fact that the maximal effect was a partial (~50%) displacement of the radioligand $[^3H]$CP55,940 in cerebellar membranes disagreed with agonist binding. Importantly, it was also first noted that hemopressin might not be endogenous but an acid extraction artifact from RVD-hemopressin (Gomes et al., 2010). In fact, D-P bonds are known to be readily hydrolyzed by acids (Che et al., 2007;

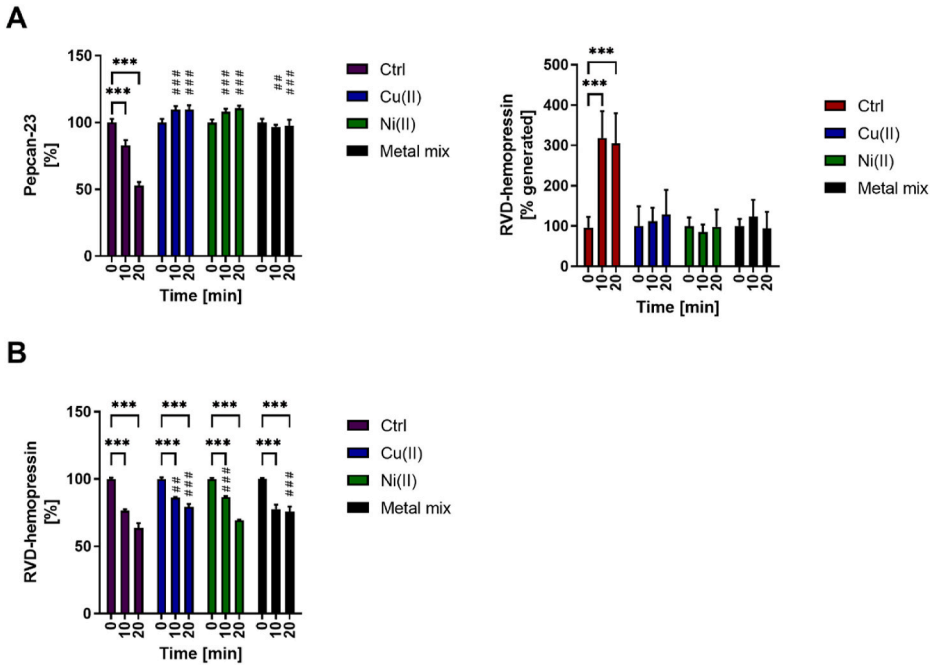

Fig. 9. Divalent metals inhibit degradation of pepcan-23 but not RVD-hemopressin. Pepcan-23 or RVD-hemopressin (2 μM) was incubated in whole blood homogenate for different time points. (**A**) Under normal conditions (control treatment, Ctrl) pepcan-23 (left) converted to RVD-hemopressin (right). Preincubation with either $CuCl_2$, $NiCl_2$ or a mixture of metals ($ZnCl_2$, $CaCl_2$, $MgCl_2$ and $MnCl_2$) (5 mM) prevented pepcan-23 conversion to RVD-hemopressin and pepcan-23 degradation. (**B**) RVD-hemopressin degradation was not fully inhibited by preincubation with divalent metals. Data show mean values ± SD from at least three independent experiments from three donors, each measured in n = 3–6. Data was analyzed with two-way ANOVA followed by Bonferroni post-hoc test. *, $p < 0.05$, **, $p < 0.01$ ***, $p < 0.001$.

Light, 1967; Marcus, 1985; Piszkiewicz et al., 1970). In 2012, using a monoclonal antibody (mAb) raised against the C-terminus of RVD-hemopressin sequence (FKLLSH as a fragment of hemopressin), we identified additional N-terminally extended peptides in different mouse tissues, but not hemopressin (Bauer et al., 2012). Because some peptides interacted with CB receptors, this family of peptides was designated peptide endocannabinoids (pepcans). Based on the length of the N-terminal amino acid sequence, they were named pepcan-12 (RVD-hemopressin) to pepcan-23, which is the largest peptide found. In our hands, pepcan-12 (mouse/human RVD-hemopressin) gave the clearest results in CB receptor binding and functional studies using cAMP and GTPγS assays and performed as an allosteric binder and NAM of CB1 receptors (Bauer et al., 2012). The NAM effect of RVD-hemopressin was independently confirmed by electrophysiology in cultured autaptic hippocampal neuronal cells measuring CB1 receptor-mediated modulation of synaptic transmission (Straiker et al., 2015). In our hands, RVD-hemopressin also potently interacted as PAM with CB2 receptors at nanomolar concentrations (Petrucci et al., 2017). The unexpected CB receptor-specific dual NAM-PAM function of this peptide observed *in vitro* inspired speculations regarding its biological role as novel ECS modulator. A biological role for RVD-hemopressin (pepcan-12) and also pepcan-23 was further suggested by the remarkably strict localization of these peptides in noradrenergic neurons and in the adrenal medulla associated with the sympathetic system (Hofer et al., 2015; Petrucci et al., 2017). We previously reported that upon adrenalectomy the amounts of RVD-hemopressin and pepcan-23 dramatically decreased (Petrucci et al., 2017). This suggested that pepcan-23 could act as pro-peptide of RVD-hemopressin. To generate experimental evidence *in vivo* for the role of pepcan-23 as pro-peptide and RVD-hemopressin as CB receptor modulator is challenging. Unfortunately, studies with hemopressins are hampered by the biological instability of these peptides and, to our knowledge, only one semi-quantitative study partially addressed the bioavailability of hemopressin to the brain (Fogaça et al., 2015). Therefore, experiments performed in mice using hemopressins need to be interpreted with caution. Several *in vivo* studies were performed using hemopressin and RVD-hemopressin (for full overview see Supplementary Table 6), but generally without addressing their biological stability or bioavailability. Among the described pharmacological actions of hemopressin are hypotensive effects in mice and rats (Blais et al., 2005) and a modulation of penicillin-induced epileptiform activity in rats (Aygun et al., 2020). Interestingly, hemopressin behaved as an antagonist of CB1 receptors (like RVD-hemopressin in our hands) in various models of pain (Heimann et al., 2007; Toniolo et al., 2014). Moreover, hemopressin exhibited anxiogenic-like effects in rats though the peptide did not cross the blood-brain barrier (Fogaça et al., 2015). Additionally, intrathecal administration of hemopressin displayed antinociceptive effects in an experimental hyperalgesia rat model (Dale et al., 2005), a neuropathic spinal cord injury pain model, and in the formalin test (Hama and Sagen, 2011a, 2011b). However, pretreatment with hemopressin could not attenuate or block the WIN55,212-2 mediated antinociceptive effect (Hama and Sagen, 2011a, 2011b). In contrast, in a dose-escalation evaluation using hemopressin in a rat model of arthritic pain, no antinociceptive effect was observed. However, upon 2-AG and hemopressin co-administration, the antinociceptive effect of 2-AG was inhibited in the same

model (Petrovszki et al., 2012). Many of the reported effects are difficult to interpret considering the findings of the present study that hemopressin is not bioavailable to tissues upon i.p. injection and RVD-hemopressin only showed partial stability *in vivo*. Thus, pharmacological experiments using these peptides require experimental control over the pharmacokinetic parameters (peptide bioavailability and metabolism) based on suitable analytical methods.

We have established a sensitive quantitative LC-ESI-MS/MS method for hemopressins and pepcan-23 (Hofer et al., 2015; Petrucci et al., 2017). With the current method, it is possible to detect and quantify hemopressins and pepcan-23 in the nanomolar range in various biological tissues with varying matrix complexity. In agreement with our previous studies (Hofer et al., 2015; Petrucci et al., 2017), our present data confirm that using a gentle extraction protocol only RVD-hemopressin and pepcan-23 are present in biological material. Since these peptides are also found in mouse brain, they are *bona fide* neuropeptides. It cannot be excluded that during the degradation of RVD-hemopressin, also smaller bioactive peptides are formed (de Araujo et al., 2019; Heimann et al, 2020, 2021), though no physiological evidence of this has been provided yet. In fact, the smaller hemopressins (e.g., VD-hemopressin) are artificial or only present in traces and may represent intermediates of RVD-hemopressin degradation (Gomes et al., 2009; Han et al., 2014; Pan et al, 2014, 2015; Zhang et al., 2016; Zheng et al., 2017). Here we measured pepcan-23 in human whole blood in absolute amounts of approximately 50 pmol/mL, mostly associated with the cellular fraction. In comparison, RVD-hemopressin levels showed a significantly higher variability between blood donors, possibly due to degradation, but maybe also because of blood sample handling. The major aim of this study was to investigate the conformation of pepcan-23, which does not bind to CB receptors, and to determine whether it is the precursor of the biologically active RVD-hemopressin. Since pepcan-23 was fully stable in plasma and serum, unlike hemopressin and RVD-hemopressin that were rapidly degraded, we assume that the specific conversion of pepcan-23 to RVD-hemopressin takes place in the cellular fraction, possibly through a cellular membrane-associated enzymatic machinery. Our data further demonstrate that pepcan-23 is converted, at least partially, to RVD-hemopressin *ex vivo* and *in vivo* in independent experiments. Moreover, these findings open new possibilities to use the more stable pro-peptide pepcan-23 as a biomarker related to pepcan expression. We have previously shown that RVD-hemopressin and pepcan-23 were upregulated upon stress and inflammation in peripheral tissues, including the liver in mice suffering from endotoxemia and IRI (Petrucci et al., 2017). We hypothesized that the enzymes responsible for the generation of RVD-hemopressin from pepcan-23 are present or upregulated in mouse tissues after IRI injury. Our current data confirm that RVD-hemopressin is preferentially generated in liver homogenates of IRI mice and to a much lower extent in normal mouse liver, suggesting a specific enzymatic processing. Furthermore, pepcan-23 was bioavailable upon i.p. injection in mice and transiently accumulated in peripheral tissues, including the blood and liver, where it was converted to RVD-hemopressin. Concomitantly, RVD-hemopressin rapidly accumulated in most peripheral tissues. Noteworthy, hemopressin was not detected in tissues and plasma upon i.p. injection after 15 min or later and therefore appears to be degraded rapidly *in vivo*. In line with a previous publication, hemopressin did not reach the brain in the present experiments (Fogaça et al., 2015). In our experiments, hemopressin was not bioavailable to any of the tissues measured, thus questioning some studies performed with hemopressin administered peripherally. Given the peptide sequence similarity and hemopressin and pepcan-23, we postulated that hemopressin may interfere with the degradation/conversion of the endogenous peptides RVD-hemopressin or pepcan-23, or that it may indirectly affect the ECS through modulation of eCBs or related lipids. We did not find evidence for the modulation of RVD-hemopressin or pepcan-23 upon hemopressin injection. The broader eCB lipidome, including N-acylethanolamines, arachidonic acid and prostaglandins, was not significantly modulated upon acute hemopressin injection. The only robust effect was observed with 1-stearoyl-2-arachidonoyl-sn-glycerol (SAG), which was increased in plasma. This trend was also seen in the brain, as well as the trend towards 2-AG modulation. Since SAG is a major diacylglycerol and is generated either through inhibition of 2-AG biosynthesis via diacylglycerol lipases (DAGLs) or from GPCR Gq or tyrosine receptor kinase signaling, it is possible that a degradation product of hemopressin exerts additional biological effects, possibly via yet unknown mechanisms as recently suggested (Heimann et al., 2021). However, we used a rather high dose (100 mg/kg), which may also explain the trend towards corticosterone increase, i.e., a specific stress response to the peptide injection vs. vehicle. Our data suggest that the degradation products of hemopressin and RVD-hemopressin are distinctly different as these peptides do not compete for the same peptidases/degradation pathways *in vivo* (i.e. no inverse correlation were observed).

We found important differences between the metabolic stability of pepcan-23 and hemopressins and show for the first time that divalent metal ions regulate the stability and conversion of this peptide *in vitro*. Although hemopressins were reported to complex divalent metal ions, the biological implications for this remained unclear. In 2016, first peptide metal-binding experiments were performed using human/mouse hemopressin (PVNFKLLSH) and RVD-hemopressin (RVDPVNFKLLSH), as well as rat hemopressin (PVNFKFLSH) (Remelli et al., 2016). Further studies, including NMR and CD spectroscopy, addressed the structural properties of hemopressin and RVD-hemopressin under physiological pH and acidic pH (Bomar et al., 2012; Emendato et al., 2018; Remelli et al., 2016; Scrima et al., 2010). Hemopressin favored a helical structure under acidic conditions, whereas RVD-hemopressin revealed a more helical structure at neutral pH (Emendato et al., 2018). The structures obtained by Emendato et al. were close to the native conformation of the two peptides in α-hemoglobin (Emendato et al., 2018). These findings were in disagreement with the study by Scrima et al., which highlighted a β-sheet structure of the rat hemopressin in a micelle environment and no defined structure under TFE conditions (Scrima et al., 2010). In our experiments, pepcan-23 exhibits distinct conformational and biochemical properties than hemopressin and RVD-hemopressin, respectively, because of the significantly longer peptide sequence and different biochemical properties. The data from CD spectroscopy with the peptides in the membrane environment mimicking solvent TFE revealed differences in their structural conformation, which may translate to differences in their metabolic stability. Pepcan-23 reaches an α-helical content of up to 45%, in agreement with *in silico* and *de novo* secondary structure predictions. Also, in the intact hemoglobin protein, pepcan-23 exhibits two α-helices. Hemopressin showed β-sheet conformations rather than α-helical structures, which partially explains the previously observed aggregation behavior (Bomar and Galande, 2013; Emendato et al., 2018; Song et al., 2015). Previous reports

showed the α-helical content of RVD-hemopressin increased in the presence of HFIP (Emendato et al., 2018). Likewise, in our experiments, in presence of TFE, RVD-hemopressin increased the α-helical content but in a lesser extend compared to pepcan-23. We believe that these differences of pepcan-23 can be translated to a potential biological regulation based on its structure.

Hemopressin and RVD-hemopressin have been analyzed by Remelli et al. for their Cu(II) and Ni(II) binding properties using CD spectroscopy and MS (Remelli et al., 2016). They suggested that metal coordination to RVD-hemopressin could play a biological role since it has a predisposition to form thermodynamically stable complexes with Cu(II) and Ni(II). However, no biological experiments were performed in this study. The authors characterized these stable complexes with less than nanomolar dissociation constants, which is surprising given the molar ratios used. Our present data show a clear difference between hemopressins and pepcan-23. Although we could confirm the peptide metal-binding for hemopressin and RVD-hemopressin with Cu(II) ions, it was less pronounced than in the case of pepcan-23. Similarly, we observed that Ni(II) ions induced slight conformational changes in hemopressin compared to RVD-hemopressin at pH 9 but, rather interestingly, no Ni(II) binding at physiological pH. The CD spectra show a clear binding to Cu(II) by shifts at 290–300 nm and a shift of the 222 nm band after both $CuCl_2$ and $NiCl_2$ incubation. Our data suggest that pepcan-23 exhibits biologically significant metal binding properties with Cu(II) and Ni(II) at pH 7.4 an 9. Because ESI-MS is a powerful method to characterize non-covalent complexes of biomacromolecules (Carlton and Schug, 2011; Drochioiu et al., 2009; Remelli et al., 2016; Volz et al., 1998) we employed mass spectrometry measurement. In the ESI-MS data, pepcan-23 forms adducts with maximally three Cu(II) and Ni(II) ions, in a concentration-dependent manner (1–1, 1 to 2, and 1–10 M ratio of peptide to metal). We envisage a possible biological role of the Cu(II) complexes given that copper can be present in some brain regions in a concentration range of 0.1–0.5 mM (Bush, 2000; Remelli et al., 2016). Copper is one of the most abundant transition metals and plays numerous biological roles (Schlosser et al., 2007). Considering our data, pepcan-23 showed enhanced stability upon divalent metal ion binding compared to RVD-hemopressin which may also reflect the biological situation.

Metal coordination of peptides can be relevant to the secondary structure of peptides and can lead to a stabilization of α-helix formation (Melino et al., 2014). This was, for instance, shown for HST5, which can bind in particular Zn(II) and Ni(II) ions, leading to a stabilized α-helical secondary structure, especially in the presence of negatively charged membranes in water/TFE mixtures (Melino et al, 1999, 2006, 2014). It is possible that metal coordination can lead to significant differences in the interaction of peptides with other macromolecules. Amino acids responsible for metal binding can be His, Arg, Lys, and Cys, which confer a change in charge under different pH environments (Moulahoum et al., 2020).

The observed degradation of pepcan-23 was prevented by preincubating the peptide with different divalent metal ions. Conversely, the degradation of RVD-hemopressin was not prevented by preincubation with divalent metal ions. Several theoretical considerations substantiate our experimental findings. First, part of the pepcan-23 sequence (SALSDL**HA**HKLRVDPVNFKLLSH) was described to be involved in Fe(II) binding in the heme coordination module (Inaba et al., 1998). Secondly, pepcan-23 exhibits several amino acids which are known to complex with divalent metal ions and are present in metal binding motives (Buongiorno and Straganz, 2013; Inaba et al., 1998; Melino et al., 2014; Tanner et al., 2001; Volz et al., 1998). For example, in literature, peptides containing Cys or His motifs, aspartic or glutamic acid are described to be typical interaction sites for Cu(II), Zn(II) and Ni(II) chelation under physiological conditions, such as zinc finger proteins or the N-terminal motif NH_2-xxH in albumin (Mallick et al., 2011; Melino et al., 2014; Volz et al., 1998). Another metal binding motif is the cupin motif, described as GX_5*HXH*$X_{3,4}$**E**X_6G (Buongiorno and Straganz, 2013; Tanner et al., 2001). In this sequence, the residues marked in italic (His) and bold (carboxylate) are important for the metal binding. This sequence exhibits similarity to the histidine-rich part in pepcan-23 (*HAH*KLRV**D**). Instead of a glutamic acid (cupin), pepcan-23 possesses an aspartic acid, clearly indicating a potential metal binding motif in pepcan-23 that is not present in hemopressins. Therefore, the observed binding of divalent metal ions appears to be a specific *in vivo* mechanism, possibly regulating the stability and conversion of pepcan-23 to RVD-hemopressin.

Overall, our study demonstrates for the first time that pepcan-23 is a pro-peptide of RVD-hemopressin, the endogenous allosteric modulator of CB receptors. We show that based on the helical structure of pepcan-23 this pro-peptide readily complexes all divalent metals, particularly nickel and copper. This metal complexation appears to serve as a biological regulatory mechanism for the conversion of this peptide to RVD-hemopressin and may furthermore explain the superior stability of this peptide *in vivo*. Given the apparent lack of tissue bioavailability of hemopressin and the rapid degradation of RVD-hemopressin *in vivo*, pepcan-23 as pro-peptide of RVD-hemopressin could be employed and administered in future animal studies.

CRediT authorship contribution statement

Sandra Glasmacher: Investigation, Conceptualization, Data curation, Visualization, Validation, Writing – original draft, preparation. **Jürg Gertsch:** Conceptualization, Methodology, Supervision, Writing – review & editing.

Acknowledgments

This research was funded by the Swiss National Science Foundation (SNFS) grant 189220. We thank Pal Pacher for providing the liver tissue of the IRI mice. We would like to acknowledge Daniele Pellegata for performing some LC-MS/MS experiments and Sacha Javor and Marc Heitz for their help with CD spectroscopy. We further thank Irene Spera and Vanessa Petrucci for their help with the *in vivo* experiments and Philip Förstner for reading the manuscript and for valuable suggestions.

Appendix A. Supplementary data

Supplementary data to this article can be found online at https://doi.org/10.1016/j.jbior.2021.100808.

References

Arunkumar, A.I., Kumar, T.K.S., Yu, C., 1997. Specificity of helix-induction by 2,2,2-trifluoroethanol in polypeptides. Int. J. Biol. Macromol. 21, 223–230. https://doi.org/10.1016/S0141-8130(97)00064-0.

Aygun, H., Arslan, G., Sen, E., Ayyildiz, M., Agar, E., 2020. Hemopressin increases penicillin-induced epileptiform activity in rats. Bratislava Med. J. 121, 37–42. https://doi.org/10.4149/BLL.

Bauer, M., Chicca, A., Tamborrini, M., Eisen, D., Lerner, R., Lutz, B., Poetz, O., Pluschke, G., Gertsch, J.J., 2012. Identification and quantification of a new family of peptide endocannabinoids (Pepcans) showing negative allosteric modulation at CB 1 receptors. J. Biol. Chem. 287, 36944–36967. https://doi.org/10.1074/jbc.M112.382481.

Blais, P.A., Côté, J., Morin, J., Larouche, A., Gendron, G., Fortier, A., Regoli, D., Neugebauer, W., Gobeil, F., 2005. Hypotensive effects of hemopressin and bradykinin in rabbits, rats and mice: a comparative study. Peptides 26, 1317–1322. https://doi.org/10.1016/j.peptides.2005.03.026.

Bomar, M.G., Galande, A.K., 2013. Modulation of the cannabinoid receptors by hemopressin peptides. Life Sci. 92, 520–524. https://doi.org/10.1016/j.lfs.2012.07.028.

Bomar, M.G., Samuelsson, S.J., Kibler, P., Kodukula, K., Galande, A.K., 2012. Hemopressin forms self-assembled fibrillar nanostructures under physiologically relevant conditions. Biomacromolecules 13, 579–583. https://doi.org/10.1021/bm201836f.

Buongiorno, D., Straganz, G.D., 2013. Structure and function of atypically coordinated enzymatic mononuclear non-heme-Fe(II) centers. Coord. Chem. Rev. 257, 541–563. https://doi.org/10.1016/j.ccr.2012.04.028.

Bush, A.I., 2000. Metals and neuroscience. Curr. Opin. Chem. Biol. 4, 184–191. https://doi.org/10.1016/S1367-5931(99)00073-3.

Camargo, L.L., Denadai-Souza, A., Yshii, L.M., Lima, C., Teixeira, S.A., Cerqueira, A.R.A., Gewehr, M.C.F., Fernandes, E.S., Schenka, A.A., Muscará, M.N., Ferro, E.S., Costa, S.K.P., 2020. The potential anti-inflammatory and anti-nociceptive effects of rat hemopressin (PVNFKFLSH) in experimental arthritis. Eur. J. Pharmacol. https://doi.org/10.1016/j.ejphar.2020.173636.

Carlton, D.D., Schug, K.A., 2011. A review on the interrogation of peptide-metal interactions using electrospray ionization-mass spectrometry. Anal. Chim. Acta 686, 19–39. https://doi.org/10.1016/j.aca.2010.11.050.

Che, F.Y., Zhang, X., Berezniuk, I., Callaway, M., Lim, J., Fricker, L.D., 2007. Optimization of neuropeptide extraction from the mouse hypothalamus. J. Proteome Res. 6, 4667–4676. https://doi.org/10.1021/pr060690r.

Chicca, A., Nicolussi, S., Bartholomäus, R., Blunder, M., Rey, A.A., Petrucci, V., Reynoso-Moreno, I.D.C., Viveros-Paredes, J.M., Gens, M.D., Lutz, B., Schiöth, H.B., Soeberdt, M., Abels, C., Charles, R.P., Altmann, K.H., Gertsch, J., 2017. Chemical probes to potently and selectively inhibit endocannabinoid cellular reuptake. Proc. Natl. Acad. Sci. Unit. States Am. 114, E5006–E5015. https://doi.org/10.1073/pnas.1704065114.

Dale, C.S., Pagano, R.D.L., Rioli, V., Hyslop, S., Giorgi, R., Ferro, E.S., 2005. Antinociceptive action of hemopressin in experimental hyperalgesia. Peptides 26, 431–436. https://doi.org/10.1016/j.peptides.2004.10.026.

de Araujo, C.B., Heimann, A.S., Remer, R.A., Russo, L.C., Colquhoun, A., Forti, F.L., Ferro, E.S., Araujo, C.B. De, Heimann, A.S., Remer, R.A., Russo, L.C., Colquhoun, A., Forti, F.L., Ferro, E.S., 2019. Intracellular peptides in cell biology and pharmacology. Biomolecules 9. https://doi.org/10.3390/biom9040150.

Dodd, G.T., Mancini, G., Lutz, B., Luckman, S.M., 2010. The peptide hemopressin acts through CB1 cannabinoid receptors to reduce food intake in rats and mice. J. Neurosci. 30, 7369–7376. https://doi.org/10.1523/JNEUROSCI.5455-09.2010.

Dodd, G.T., Worth, A.A., Hodkinson, D.J., Srivastava, R.K., Lutz, B., Williams, S.R., Luckman, S.M., 2013. Central functional response to the novel peptide cannabinoid, hemopressin. Neuropharmacology 71, 27–36. https://doi.org/10.1016/j.neuropharm.2013.03.007.

Drochioiu, G., Manea, M., Dragusanu, M., Murariu, M., Dragan, E.S., Petre, B.A., Mezo, G., Przybylski, M., 2009. Interaction of β-amyloid(1-40) peptide with pairs of metal ions: an electrospray ion trap mass spectrometric model study. Biophys. Chem. 144, 9–20. https://doi.org/10.1016/j.bpc.2009.05.008.

El Swefy, S., Hasan, R.A., Ibrahim, A., Mahmoud, M.F., 2016. Curcumin and hemopressin treatment attenuates cholestasis-induced liver fibrosis in rats: role of CB1 receptors. Naunyn-Schmiedeberg's Arch. Pharmacol. 389, 103–116. https://doi.org/10.1007/s00210-015-1181-7.

Emendato, A., Guerrini, R., Marzola, E., Wienk, H., Boelens, R., Leone, S., Picone, D., 2018. Disordered peptides looking for their native environment: structural basis of CB1 endocannabinoid receptor binding to pepcans. Front. Mol. Biosci. 5, 1–9. https://doi.org/10.3389/fmolb.2018.00100.

Ferrante, C., Recinella, L., Leone, S., Chiavaroli, A., Di Nisio, C., Martinotti, S., Mollica, A., Macedonio, G., Stefanucci, A., Dvorácskó, S., Tömböly, C., De Petrocellis, L., Vacca, M., Brunetti, L., Orlando, G., 2017. Anorexigenic effects induced by RVD-hemopressin(α) administration. Pharmacol. Rep. 69, 1402–1407. https://doi.org/10.1016/j.pharep.2017.05.015.

Fogaça, M.V., Sonego, A.B., Rioli, V., Gozzo, F.C., Dale, C.S., Ferro, E.S., Guimarães, F.S., 2015. Anxiogenic-like effects induced by hemopressin in rats. Pharmacol. Biochem. Behav. 129, 7–13. https://doi.org/10.1016/j.pbb.2014.11.013.

Gachet, M.S., Rhyn, P., Bosch, O.G., Quednow, B.B., Gertsch, J., 2015. A quantitative LC-MS/MS method for the measurement of arachidonic acid, prostanoids, endocannabinoids, N-acylethanolamines and steroids in human plasma. J. Chromatogr. B 976–977, 6–18. https://doi.org/10.1016/j.jchromb.2014.11.001.

Garnier, J., Osguthorpe, D.J., Robson, B., 1978. Analysis of the accuracy and implications of simple methods for predicting the secondary structure of globular proteins. J. Mol. Biol. 120, 97–120. https://doi.org/10.1016/0022-2836(78)90297-8.

Gelman, J.S., Fricker, L.D., 2010. Hemopressin and other bioactive peptides from cytosolic proteins: are these non-classical neuropeptides? AAPS J. 12, 279–289. https://doi.org/10.1208/s12248-010-9186-0.

Gomes, I., Dale, C.S., Casten, K., Geigner, M.A., Gozzo, F.C., Ferro, E.S., Heimann, A.S., Devi, L.A., 2010. Hemoglobin-derived peptides as novel type of bioactive signaling molecules. AAPS J. 12, 658–669. https://doi.org/10.1208/s12248-010-9217-x.

Gomes, I., Grushko, J.S., Golebiewska, U., Hoogendoorn, S., Gupta, A., Heimann, A.S., Ferro, E.S., Scarlata, S., Fricker, L.D., Devi, L.A., 2009. Novel endogenous peptide agonists of cannabinoid receptors. FASEB J 23, 3020–3029. https://doi.org/10.1096/fj.09-132142.

Gonzalez, P., Bossak, K., Stefaniak, E., Hureau, C., Raibaut, L., Bal, W., Faller, P., Gonzalez, P., Bossak, K., Stefaniak, E., Hureau, C., Raibaut, L., 2018. N-terminal Cu-binding motifs (Xxx-Zzz-His, Xxx-His) and their derivatives: chemistry, biology and medicinal applications. Chemistry (Easton). 24, 8029–8041. https://doi.org/10.1002/chem.201705398.

Hama, A., Sagen, J., 2011a. Centrally mediated antinociceptive effects of cannabinoid receptor ligands in rat models of nociception. Pharmacol. Biochem. Behav. 100, 340–346. https://doi.org/10.1016/j.pbb.2011.09.004.

Hama, A., Sagen, J., 2011b. Activation of spinal and supraspinal cannabinoid-1 receptors leads to antinociception in a rat model of neuropathic spinal cord injury pain. Brain Res. 1412, 44–54. https://doi.org/10.1016/j.brainres.2011.07.031.

Han, Z.L., Fang, Q., Wang, Z.L., Li, X.H., Li, N., Chang, X.M., Pan, J.X., Tang, H.Z., Wang, R., 2014. Antinociceptive effects of central administration of the endogenous cannabinoid receptor type 1 agonist VDPVNFKLLSH-OH [(m)VD-hemopressin(α)], an N-terminally extended hemopressin peptide. J. Pharmacol. Exp. Therapeut. 348, 316–323. https://doi.org/10.1124/jpet.113.209866.

Heimann, A.S., Dale, C.S., Guimarães, F.S., Reis, R.A.M., Navon, A., Shmuelov, M.A., Rioli, V., Gomes, I., Devi, L.L., Ferro, E.S., 2021. Hemopressin as a breakthrough for the cannabinoid field. Neuropharmacology 183, 108406. https://doi.org/10.1016/j.neuropharm.2020.108406.

Heimann, A.S., Giardini, A.C., Sant'Anna, M.B., Dos Santos, N.B., Gewehr, M.C.F., Munhoz, C.D., Castro, L.M., Picolo, G., Remer, R.A., Ferro, E.S., 2020. NFKF is a synthetic fragment derived from rat hemopressin that protects mice from neurodegeneration. Neurosci. Lett. 721, 134765. https://doi.org/10.1016/j.neulet.2020.134765.

Heimann, A.S., Gomes, I., Dale, C.S., Pagano, R.L., Gupta, A., De Souza, L.L., Luchessi, A.D., Castro, L.M., Giorgi, R., Rioli, V., Ferro, E.S., Devi, L.A., Robert Lefkowitz, by J., 2007. Hemopressin is an inverse agonist of CB1 cannabinoid receptors. Proc. Natl. Acad. Sci. Unit. States Am. 104, 20588–20593. https://doi.org/10.1073/pnas.0706980105.

Hofer, S.C., Ralvenius, W.T., Gachet, M.S., Fritschy, J.M., Zeilhofer, H.U., Gertsch, J., 2015. Localization and production of peptide endocannabinoids in the rodent CNS and adrenal medulla. Neuropharmacology 98, 78–89. https://doi.org/10.1016/j.neuropharm.2015.03.021.

Inaba, K., Ishimori, K., Morishima, I., 1998. Structural and functional roles of heme binding module in globin proteins: identification of the segment regulating the heme binding structure. J. Mol. Biol. 283, 311–327. https://doi.org/10.1006/jmbi.1998.2073.

Lamiable, A., Thévenet, P., Rey, J., Vavrusa, M., Derreumaux, P., Tufféry, P., 2016. PEP-FOLD3: faster de novo structure prediction for linear peptides in solution and in complex. Nucleic Acids Res. 44, W449–W454. https://doi.org/10.1093/nar/gkw329.

Lenman, A., Fowler, C.J., 2007. Interaction of ligands for the peroxisome proliferator-activated receptor γ with the endocannabinoid system. Br. J. Pharmacol. 151, 1343–1351. https://doi.org/10.1038/sj.bjp.0707352.

Leone, S., Recinella, L., Chiavaroli, A., Martinotti, S., Ferrante, C., Mollica, A., Macedonio, G., Stefanucci, A., Dvorácskó, S., Tömböly, C., De Petrocellis, L., Vacca, M., Brunetti, L., Orlando, G., 2017. Emotional disorders induced by Hemopressin and RVD-hemopressin(α) administration in rats. Pharmacol. Rep. 69, 1247–1253. https://doi.org/10.1016/j.pharep.2017.06.010.

Li, X.H., Lin, M.L., Wang, Z.L., Wang, P., Tang, H.H., Lin, Y.Y., Li, N., Fang, Q., Wang, R., 2016. Central administrations of hemopressin and related peptides inhibit gastrointestinal motility in mice. Neuro Gastroenterol. Motil. 28, 891–899. https://doi.org/10.1111/nmo.12789.

Light, A., 1967. Partial acid hydrolysis. Methods Enzymol. 11, 417–420. https://doi.org/10.1016/S0076-6879(67)11048-3.

Lippton, H., Lin, B., Gumusel, B., Witriol, N., Wasserman, A., Knight, M., 2006. Hemopressin, a hemoglobin fragment, dilates the rat systemic vascular bed through release of nitric oxide. Peptides 27, 2284–2288. https://doi.org/10.1016/j.peptides.2006.04.010.

Lobley, A., Whitmore, L., Wallace, B.A., 2002. DICHROWEB: an interactive website for the analysis of protein secondary structure from circular dichroism spectra. Bioinformatics 18, 211–212. https://doi.org/10.1093/bioinformatics/18.1.211.

Mahmoud, M.F., Swefy, S. El, Hasan, R.A., Ibrahim, A., 2014. Role of cannabinoid receptors in hepatic fibrosis and apoptosis associated with bile duct ligation in rats. Eur. J. Pharmacol. 742, 118–124. https://doi.org/10.1016/j.ejphar.2014.08.021.

Mallick, M., Sharan Vidyarthi, A., Shankaracharya, 2011. Tools for predicting metal binding sites in protein: a review. Curr. Bioinf. 6, 444–449. https://doi.org/10.2174/157489311798072990.

Marcus, F., 1985. Preferential cleavage at aspartyl-prolyl peptide bonds in dilute acid. Int. J. Pept. Protein Res. 25, 542–546. https://doi.org/10.1111/j.1399-3011.1985.tb02208.x.

Matsuda, L.A., Lolait, S.J., Brownstein, M.J., Young, A.C., Bonner, T.I., 1990. Structure of a cannabinoid receptor and functional expression of the cloned cDNA. Nature 346, 561–564. https://doi.org/10.1038/346561a0.

Mechoulam, R., Gaoni, Y., 1964. Hashish-IV. The isolation and structure of cannabinolic cannabidiolic and cannabigerolic acids. Tetrahedron 21, 1223–1229. https://doi.org/10.1016/0040-4020(65)80064-3.

Mechoulam, R., Parker, L.A., 2013. The endocannabinoid system and the brain. Annu. Rev. Psychol. 64, 21–47. https://doi.org/10.1146/annurev-psych-113011-143739.

Melino, S., Gallo, M., Trotta, E., Mondello, F., Paci, M., Petruzzelli, R., 2006. Metal-binding and nuclease activity of an antimicrobial peptide analogue of the salivary histatin 5. Biochemistry 45, 15373–15383. https://doi.org/10.1021/bi0615137.

Melino, S., Rufini, S., Sette, M., Morero, R., Grottesi, A., Paci, M., Petruzzelli, R., 1999. Zn2+ ions selectively induce antimicrobial salivary peptide histatin- 5 to fuse negatively charged vesicles. Identification and characterization of a zinc-binding motif present in the functional domain. Biochemistry 38, 9626–9633. https://doi.org/10.1021/bi990212c.

Melino, S., Santone, C., Di Nardo, P., Sarkar, B., 2014. Histatins: salivaryx peptides with copper(II)- and zinc(II)-binding motifs Perspectives for biomedical applications. FEBS J. 281, 657–672. https://doi.org/10.1111/febs.12612.

Morales, P., Hurst, D.P., Reggio, P.H., 2017. Molecular targets of the phytocannabinoids: a complex picture. Phytocannabinoids 103. https://doi.org/10.1007/978-3-319-45541-9, 1266–1266.

Moulahoum, H., Ghorbani Zamani, F., Timur, S., Zihnioglu, F., 2020. Metal binding antimicrobial peptides in nanoparticle bio-functionalization: new Heights in drug delivery and therapy. Probiotics Antimicrob. Proteins 12, 48–63. https://doi.org/10.1007/s12602-019-09546-5.

Pan, J.X., Wang, Z.L., Li, N., Han, Z.L., Li, X.H., Tang, H.H., Wang, P., Zheng, T., Fang, Q., Wang, R., 2014. Analgesic tolerance and cross-tolerance to the cannabinoid receptors ligands hemopressin, VD-hemopressin(α) and WIN55,212-2 at the supraspinal level in mice. Neurosci. Lett. 578, 187–191. https://doi.org/10.1016/j.neulet.2014.06.058.

Pan, J.X., Wang, Z.L., Li, N., Zhang, N., Wang, P., Tang, H.H., Zhang, T., Yu, H.P., Zhang, R., Zheng, T., Fang, Q., Wang, R., 2015. Effects of neuropeptide FF and related peptides on the antinociceptive activities of VD-hemopressin(α) in naive and cannabinoid-tolerant mice. Eur. J. Pharmacol. 767, 119–125. https://doi.org/10.1016/j.ejphar.2015.10.016.

Petrovszki, Z., Kovacs, G., Tömböly, C., Benedek, G., Horvath, G., 2012. The effects of peptide and lipid endocannabinoids on arthritic pain at the spinal level. Anesth. Analg. 114, 1346–1352. https://doi.org/10.1213/ANE.0b013e31824c4eeb.

Petrucci, V., Chicca, A., Glasmacher, S., Paloczi, J., Cao, Z., Pacher, P., Gertsch, J., 2017. Pepcan-12 (RVD-hemopressin) is a CB2 receptor positive allosteric modulator constitutively secreted by adrenals and in liver upon tissue damage. Sci. Rep. 7, 1–14. https://doi.org/10.1038/s41598-017-09808-8.

Piszkiewicz, D., Landon, M., Smith, E.L., 1970. Anomalous cleavage of aspartyl-proline peptide bonds during amino acid sequence determinations. Biochem. Biophys. Res. Commun. 40, 1173–1178. https://doi.org/10.1016/0006-291X(70)90918-6.

Prevelige, P., Fasman, G.D., 1989. Chou-fasman prediction of the secondary structure of proteins. Predict. protein Struct. Princ. protein Conform. 391–416. https://doi.org/10.1016/b978-0-12-397580-5.50041-7.

Provencher, S.W., Glöckner, J., 1981. Estimation of globular protein secondary structure from circular dichroism. Biochemistry 20, 33–37. https://doi.org/10.1021/bi00504a006.

Recinella, L., Chiavaroli, A., Ferrante, C., Mollica, A., Macedonio, G., Stefanucci, A., Dimmito, M.P., Dvorácskó, S., Tömböly, C., Brunetti, L., Orlando, G., Leone, S., 2018. Effects of central RVD-hemopressin(α) administration on anxiety, feeding behavior and hypothalamic neuromodulators in the rat. Pharmacol. Rep. 70, 650–657. https://doi.org/10.1016/j.pharep.2018.01.010.

Remelli, M., Ceciliato, C., Guerrini, R., Kolkowska, P., Krzywoszynska, K., Salvadori, S., Valensin, D., Watly, J., Kozlowski, H., 2016. Does hemopressin bind metal ions in vivo? Dalton Trans. 45, 18267–18280. https://doi.org/10.1039/C6DT03598A.

Rioli, V., Gozzo, F.C., Heimann, A.S., Linardi, A., Krieger, J.E., Shida, C.S., Almeida, P.C., Hyslop, S., Eberlin, M.N., Ferro, E.S., Krieger, E., Shida, S., Almeida, P.C., Hyslop, S., Eberlin, M.N., Krieger, J.E., Shida, C.S., Almeida, P.C., Hyslop, S., Eberlin, M.N., Ferro, E.S., 2003. Novel natural peptide substrates for endopeptidase 24.15, neurolysin, and angiotensin-converting enzyme. J. Biol. Chem. 278, 8547–8555. https://doi.org/10.1074/jbc.M212030200.

Roccatano, D., Colombo, G., Fioroni, M., Mark, A.E., 2002. Mechanism by which 2,2,2-trifluoroethanol/water mixtures stabilize secondary-structure formation in peptides: a molecular dynamics study. Proc. Natl. Acad. Sci. Unit. States Am. 99, 12179–12184. https://doi.org/10.1073/pnas.182199699.

Ryberg, E., Larsson, N., Sjögren, S., Hjorth, S., Hermansson, N.O., Leonova, J., Elebring, T., Nilsson, K., Drmota, T., Greasley, P.J., 2007. The orphan receptor GPR55 is a novel cannabinoid receptor. Br. J. Pharmacol. 152, 1092–1101. https://doi.org/10.1038/sj.bjp.0707460.

Schlosser, G., Stefanescu, R., Przybylski, M., Murariu, M., Hudecz, F., Drochioiu, G., 2007. Copper-induced oligomerization of peptides: a model study. Eur. J. Mass Spectrom. 13, 331–337. https://doi.org/10.1255/ejms.889.

Schuele, L.-L., Glasmacher, S., Gertsch, J., Roggan, M.D., Transfeld, J.-L., Bindila, L., Lutz, B., Kolbe, C.-C., Bilkei-Gorzo, A., Zimmer, A., Leidmaa, E., 2020. Diacylglycerol lipase alpha in astrocytes is involved in maternal care and affective behaviors. Glia 1–15. https://doi.org/10.1002/glia.23903.

Scrima, M., Di Marino, S., Grimaldi, M., Mastrogiacomo, A., Novellino, E., Bifulco, M., D'Ursi, A.M., 2010. Binding of the hemopressin peptide to the cannabinoid CB1 receptor: structural insights. Biochemistry 49, 10449–10457. https://doi.org/10.1021/bi1011833.

Sigel, E., Baur, R., Rácz, I., Marazzi, J., Smart, T.G., Zimmer, A., Gertsch, J., 2011. The major central endocannabinoid directly acts at GABA A receptors. Proc. Natl. Acad. Sci. U.S.A. 108, 18150–18155. https://doi.org/10.1073/pnas.1113444108.

Song, B., Kibler, P.D., Endsley, A.N., Nayak, S.K., Galande, A.K., Jambunathan, K., 2015. Site-specific substitutions eliminate aggregation properties of hemopressin. Chem. Biol. Drug Des. 86, 1433–1437. https://doi.org/10.1111/cbdd.12610.

Sönnichsen, F.D., Van Eyk, J.E., Hodges, R.S., Sykes, B.D., 1992. Effect of trifluoroethanol on protein secondary structure: an NMR and CD study using a synthetic actin peptide. Biochemistry 31, 8790–8798. https://doi.org/10.1021/bi00152a015.

Straiker, A., Mitjavila, J., Yin, D., Gibson, A., Mackie, K., 2015. Aiming for allosterism: evaluation of allosteric modulators of CB1 in a neuronal model. Pharmacol. Res. 99, 370–376. https://doi.org/10.1016/j.phrs.2015.07.017.

Tamburro, A.M., Scatturin, A., Rocchi, R., Marchiori, F., Borin, G., Scoffone, E., 1968. Conformational-transitions of bovine pancreatic ribonuclease S-peptide. FEBS Lett. 1, 298–300. https://doi.org/10.1016/0014-5793(68)80137-1.

Tanaka, K., Shimizu, T., Yanagita, T., Nemoto, T., Nakamura, K., Taniuchi, K., Dimitriadis, F., Yokotani, K., Saito, M., 2014. Brain RVD-haemopressin, a haemoglobin-derived peptide, inhibits bombesin-induced central activation of adrenomedullary outflow in the rat. Br. J. Pharmacol. 171, 202–213. https://doi.org/10.1111/bph.12471.

Tanner, A., Bowater, L., Fairhurst, S.A., Bornemann, S., 2001. Oxalate decarboxylase requires manganese and dioxygen for activity: overexpression and characterization of Bacillus subtilis YvrK and YoaN. J. Biol. Chem. 276, 43627–43634. https://doi.org/10.1074/jbc.M107202200.

Thakare, R., Chhonker, Y.S., Gautam, N., Alamoudi, J.A., Alnouti, Y., 2016. Quantitative analysis of endogenous compounds. J. Pharmaceut. Biomed. Anal. 128, 426–437. https://doi.org/10.1016/j.jpba.2016.06.017.

Thévenet, P., Shen, Y., Maupetit, J., Guyon, F., Derreumaux, P., Tufféry, P., 2012. PEP-FOLD: an updated de novo structure prediction server for both linear and disulfide bonded cyclic peptides. Nucleic Acids Res. 40, 288–293. https://doi.org/10.1093/nar/gks419.

Toniolo, E.F., Maique, E.T., Ferreira, W.A., Heimann, A.S., Ferro, E.S., Ramos-Ortolaza, D.L., Miller, L., Devi, L.A., Dale, C.S., 2014. Hemopressin, an inverse agonist of cannabinoid receptors, inhibits neuropathic pain in rats. Peptides 56, 125–131. https://doi.org/10.1016/j.peptides.2014.03.016.

Van Stokkum, I.H., Spoelder, H.J., Bloemendal, M., Van Grondelle, R., Groen, F.C., 1990. Estimation of protein secondary structure and error analysis from circular dichroism spectra. Anal. Biochem. 191, 110–118. https://doi.org/10.5220/0002478200580067.

Volz, J., Uwe Bosch, F., Wunderlin, M., Schuhmacher, M., Melchers, K., Bensch, K., Steinhilber, W., Schäfer, K.P., Tóth, G., Penke, B., Przybylski, M., 1998. Molecular characterization of metal-binding polypeptide domains by electrospray ionization mass spectrometry and metal chelate affinity chromatography. J. Chromatogr. A 800, 29–37. https://doi.org/10.1016/S0021-9673(97)00877-7.

Wei, F., Zhao, L., Jing, Y., 2020. Signaling molecules targeting cannabinoid receptors: hemopressin and related peptides. Neuropeptides 79, 101998. https://doi.org/10.1016/j.npep.2019.101998.

Whitmore, L., Wallace, B.A., 2008. Protein secondary structure analyses from circular dichroism spectroscopy: methods and reference databases. Biopolymers 89, 392–400. https://doi.org/10.1002/bip.20853.

Whitmore, L., Wallace, B.A., 2004. DICHROWEB, an online server for protein secondary structure analyses from circular dichroism spectroscopic data. Nucleic Acids Res. 32, 668–673. https://doi.org/10.1093/nar/gkh371.

Yang, J., Zhang, Y., 2015. I-TASSER server: new development for protein structure and function predictions. Nucleic Acids Res. 43, W174–W181. https://doi.org/10.1093/nar/gkv342.

Yévenes, G.E., Zeilhofer, H.U., 2011. Molecular sites for the positive allosteric modulation of glycine receptors by endocannabinoids. PloS One 6. https://doi.org/10.1371/journal.pone.0023886.

Zhang, C., Freddolino, P.L., Zhang, Y., 2017a. COFACTOR: improved protein function prediction by combining structure, sequence and protein-protein interaction information. Nucleic Acids Res. 45, W291–W299. https://doi.org/10.1093/nar/gkx366.

Zhang, R., He, Z., Jin, W., Wang, R., 2016. Effects of the cannabinoid 1 receptor peptide ligands hemopressin RVD-hemopressin(α) and (m)VD-hemopressin(α) on memory in novel object and object location recognition tasks in normal young and Aβ1–42-treated mice. Neurobiol. Learn. Mem. 134, 264–274. https://doi.org/10.1016/j.nlm.2016.07.030.

Zheng, T., Zhang, T., Zhang, R., Wang, Z.L., Han, Z.L., Li, N., Li, X.H., Zhang, M.N., Xu, B., Yang, X.L., Fang, Q., Wang, R., 2017b. Pharmacological characterization of rat VD-hemopressin(α), an α-hemoglobin-derived peptide exhibiting cannabinoid agonist-like effects in mice. Neuropeptides 63, 83–90. https://doi.org/10.1016/j.npep.2016.12.006.

Zhou, L., Jin, Q., Yang, Y., Liu, Z., Li, X., Dong, S., Zhao, L., 2012. Effects of endokinin A/B and endokinin C/D on the antinociception properties of hemopressin in mice. Peptides 38, 70–80. https://doi.org/10.1016/j.peptides.2012.08.006.

Zygmunt, P.M., Petersson, J., Andersson, D.A., Chuang, H.H., Sørgård, M., Di Marzo, V., Julius, D., Högestätt, E.D., 1999. Vanilloid receptors on sensory nerves mediate the vasodilator action of anandamide. Nature 400, 452–457. https://doi.org/10.1038/22761.